SUPPLEMENTARY MATERIAL

Ultra-high performance liquid chromatography - high resolution mass spectrometry profiling and hepatoprotective activity of purified saponin and flavonoid fractions from the aerial parts of wild spinach (*Chenopodium bonus-henricus* L.)

Zlatina Kokanova-Nedialkova[1]*, Paraskev Nedialkov[1]*, Magdalena Kondeva-Burdina[2]

[1]Department of Pharmacognosy, Faculty of Pharmacy, Medical University of Sofia,

2 Dunav Str., 1000 Sofia, Bulgaria

[2]Laboratory of drug metabolism and drug toxicity, Department of Pharmacology, Pharmacotherapy and Toxicology, Faculty of Pharmacy, Medical University of Sofia, 2 Dunav Str., 1000 Sofia, Bulgaria

***Corresponding authors: Zlatina Kokanova-Nedialkova**, **Paraskev Nedialkov**, Department of Pharmacognosy, Faculty of Pharmacy, Medical University of Sofia, 2 Dunav Str., 1000 Sofia, Bulgaria

E-mails: zlatina.kokanova@pharmfac.mu-sofia.bg, pnedialkov@pharmfac.mu-sofia.bg.

Abstract: A ultra-high performance liquid chromatography - high resolution mass spectrometry profiling method was used for a comprehensive study of flavonoid and saponin-rich fractions from the aerial parts of wild spinach (*Chenopodium bonus-henricus* L.). Thirty-six compounds, respectively **22** saponins of eight sapogenins (phytolaccagenin, bayogenin, medicagenic acid, 2*β*-hydroxygypsogenin, 2*β*-hydroxyoleanoic acid, 2-hydroxy-30-nor-gypsogenin, 2-hydroxyakebonic acid, and akebonic acid) together with **12** flavonoid glycosides of 6-methoxykaempferol, isorhamnetin, patuletin, spinacetin as well as two ecdysteroids (20-hydroxyecdysone and polypodine B) were detected. The occurrence of sapogenins 2-hydroxy-30-nor-gypsogenin, 2-hydroxyakebonic acid, and akebonic acid in the *Chenopodium* genus is reported here for the first time. The flavonoid and saponin-rich fractions showed *in vitro* hepatoprotective and antioxidant activity comparable to those of flavonoid complex silymarin (60 μg/mL) in a model of metabolic bioactivation, induced by CCl_4. All tested fractions, compared to silymarin, significantly reduced the cellular damage caused by CCl_4 in rat hepatocytes, preserved cell viability and GSH level, decreased LDH leakage, and reduced lipid damage. The results showed that saponin-rich fractions F3A and F3B possessed better hepatoprotective activity than flavonoid-rich fractions (F2A and F2B). The most active was fraction F3B and this is probably due to the synergism between the saponins and some acylated flavonol glycosides found there.

Keywords: *Chenopodium bonus-henricus*, Amaranthaceae, UHPLC-HRMS, hepatoprotective activity

Table of Contents

Table S1: Characterization of flavonoids of the aerial parts of *C. bonus-henricus* L. in the negative ion mode.

No.	t_R[1] (min)	Frs[2]	Identification	Ion mode	Found *m/z*	Composition (δ ppm)
1[3]	7.57	F2A F2B	Patuletin-3-O-[*β*-Api(1→2)] -*β*-Glu (1→6)-*β*-Glu	$[M–H]^-$	787.1923	$C_{33}H_{39}O_{22}$ (-0.54)
2[3]	8.49	F2A F2B F3B	Patuletin-3-O-*β*-Glu(1→6)-*β*-Glu	$[M–H]^-$	655.1515	$C_{28}H_{31}O_{18}$ (1.53)
3	8.83	F2A F2B	Isorhamnetin-Hex-Hex-Pent	$[M–H]^-$	771.1984	$C_{33}H_{39}O_{21}$ (0.77)
4[3]	8.94	F2A F2B	6-methoxykaempferol-3-O-[*β*-Api (1→2)]-*β*-Glu (1→6)-*β*-Glu	$[M–H]^-$	771.1980	$C_{33}H_{39}O_{21}$ (0.21)
5[3]	9.41	F2A F2B	Spinacetin-3-O-[*β*-Api (1→2)]-*β*-Glu (1→6)-*β*-Glu	$[M–H]^-$	801.2080	$C_{34}H_{41}O_{22}$ (-0.49)
6[3]	10.40	F2A F2B F3B	6-methoxykaempferol-3-O-*β*-Glu(1→6)-*β*-Glu	$[M–H]^-$	639.1567	$C_{28}H_{31}O_{17}$ (1.73)
7	10.50	F2A F2B	Isorhamnetin-Hex-Hex	$[M–H]^-$	639.1570	$C_{28}H_{31}O_{17}$ (2.20)
10[3]	11.09	F2A F2B F3B	Spinacetin-3-O-*β*-Glu(1→6)-*β*-Glu	$[M–H]^-$	669.1671	$C_{29}H_{33}O_{18}$ (1.45)
11[3]	14.28	F2B	Patuletin-3-O-(5‴-O-E-FA)-*β*-D-Api (1→2) [*β*-D-Glu(1→6)]-*β*-D-Glu	$[M–H]^-$	963.2390	$C_{43}H_{47}O_{25}$ (-1.19)
12	15.74	F2B	Isorhamnetin-Hex-Hex-Pent-FA	$[M–H]^-$	947.2468	$C_{43}H_{47}O_{24}$ (1.68)
13[3]	15.82	F2B F3A[4] F3B	Spinacetin-3-O-(5‴-O-*E*-FA)-*β*-D-Api (1→2)[*β*-D-Glu (1→6)]-*β*-D-Glu	$[M–H]^-$	977.2520	$C_{44}H_{49}O_{25}$ (-3.82)
14[3]	16.17	F2B F3B	6-methoxykaempferol-3-O-(5‴-O-E-FA)-*β*-D-Api (1→2)[*β*-D-Glu (1→6)]-*β*-D-Glu	$[M–H]^-$	947.2451	$C_{43}H_{47}O_{24}$ (0.06)

[1] t_R - retention time of detected compounds in the MeOH extract.

[2] Fraction containing the compound.

[3] Flavonoids compared with a reference compound.

[4] The compounds were in trace.

Api, apiose; Glu, glucose; FA, ferulic acid; Pent, pentose; Hex, hexose.

Table S2: Effects of co-administration of fractions F2A, F2B, F3A, F3B and silymarin complex (S)(60 μg/mL) with CCl_4 on the parameters, which characterized functional-metabolic status of isolated rat hepatocytes.

Group	**Cell viability (%)**		**LDH activity (μmol/min/10^6 cells)**		**GSH level (nmol/10^6 cells)**		**MDA level (nmol/10^6 cells)**	
Control	85 ± 5.2		0.102 ± 0.01		18 ± 2.8		0.052 ± 0.01	
86 μM CCl_4	32 ± 4.8[a]	↓62*	0.423 ± 0.02[a]	↑315*	5 ± 2.3[a]	↓72*	0.253 ± 0.01[a]	↑387*
F2A + CCl_4	55 ± 6.2[b]	↑72**	0.313 ± 0.02[b]	↓26**	10 ± 3.2[b]	↑100**	0.171 ± 0.01[b]	↓32**
F2B + CCl_4	52 ± 3.8[b]	↑63**	0.328 ± 0.01[b]	↓22**	10 ± 4.2[b]	↑100**	0.178 ± 0.02[b]	↓30**
F3A + CCl_4	58 ± 3.9[b]	↑81**	0.318 ± 0.01[b]	↓25**	12 ± 2.1[b]	↑140**	0.160 ± 0.02[b]	↓37**
F3B + CCl_4	66 ± 4.2[b]	↑106**	0.231 ± 0.01[b]	↓45**	15 ± 5.2[b]	↑200**	0.124 ± 0.01[b]	↓51**
S + CCl_4	66 ± 3.1[b]	↑106**	0.225 ± 0.01[b]	↓47**	15 ± 4.1[b]	↑200**	0.121 ± 0.01[b]	↓52**

Significance levels: [a]$p < 0.001$ vs. control; [b]$p < 0.001$ vs. CCl_4.

* Effect vs control (%)

** Effect vs CCl_4 (%)

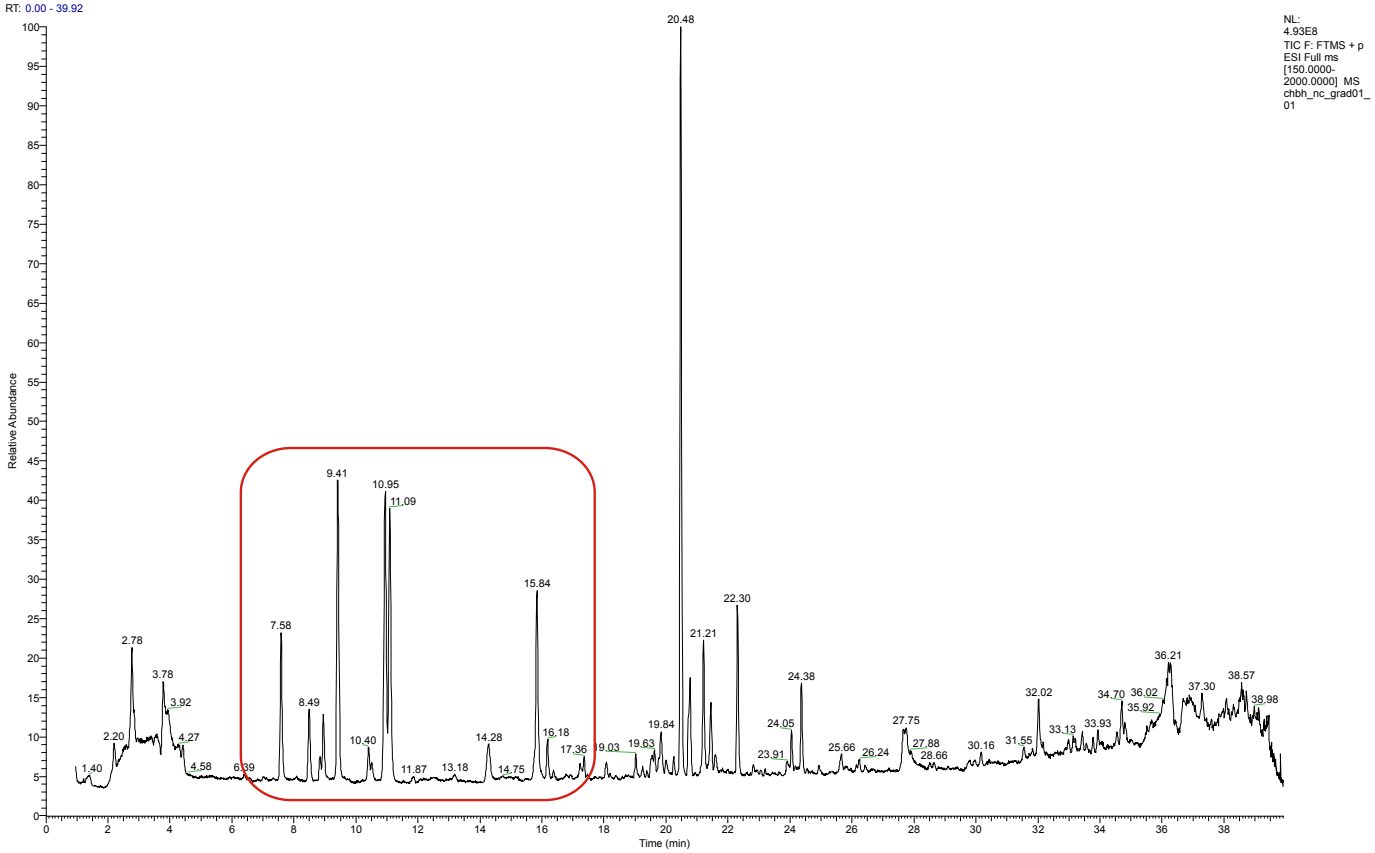

Figure S1: UHPLC-HRMS based profiling of MeOH extract from the aerial parts of *C. bonus-henricus* L. in the positive ion mode and detected flavonoids and ecdysteroids

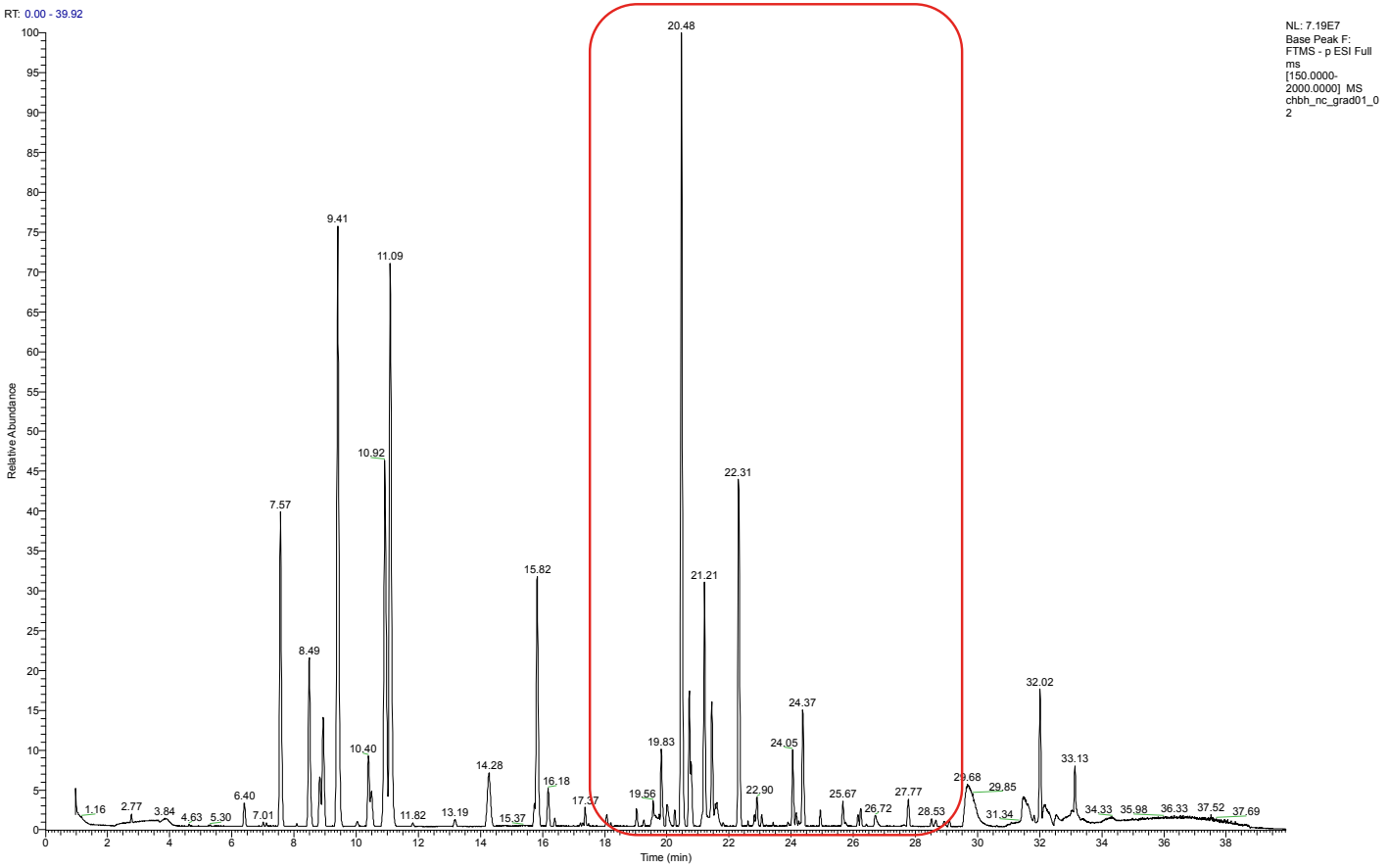

Figure S2: UHPLC-HRMS based profiling of MeOH extract from the aerial parts of *C. bonus-henricus* L. in the negative ion mode and detected saponin

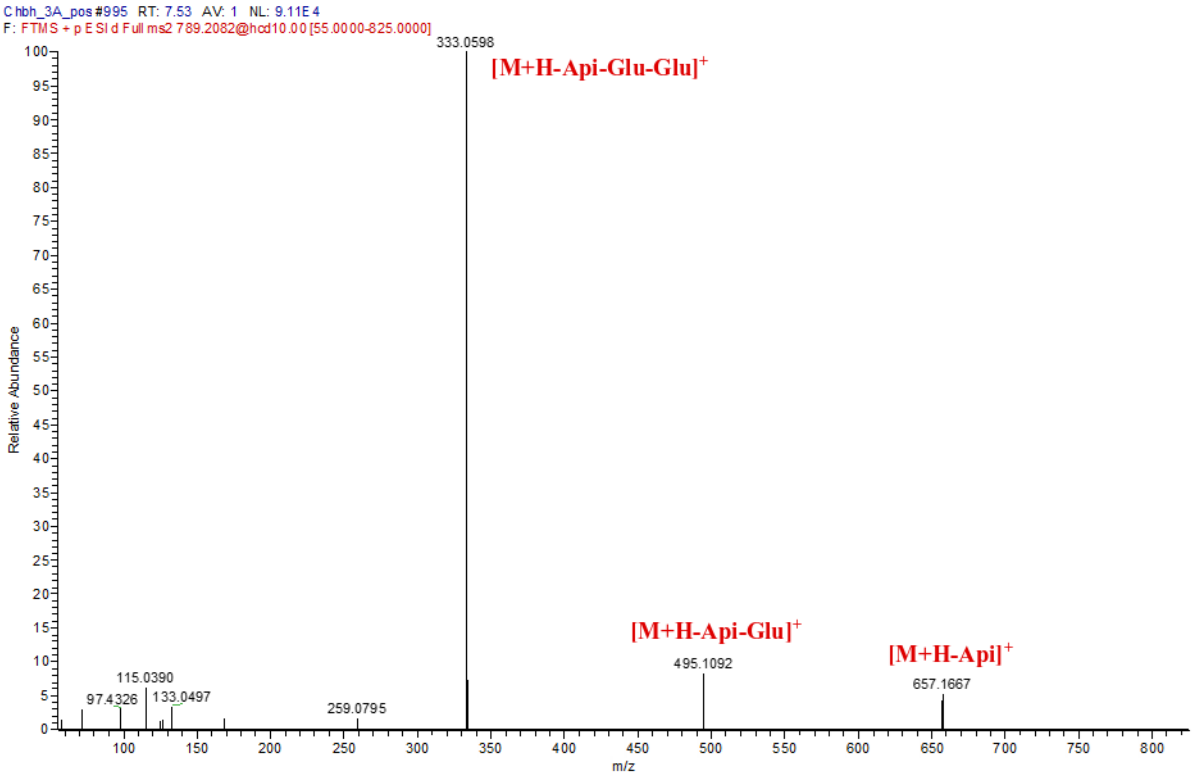

Figure S3: MS^2 spectrum of Compound **1**

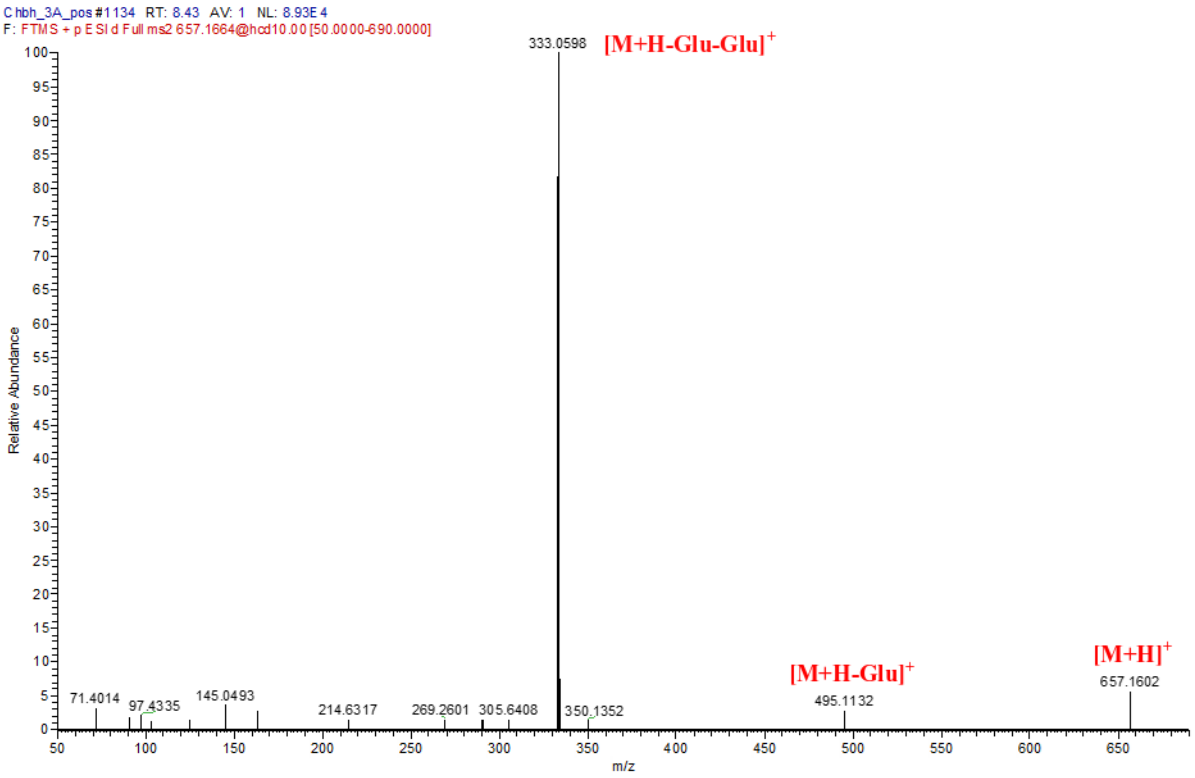

Figure S4: MS^2 spectrum of Compound **2**

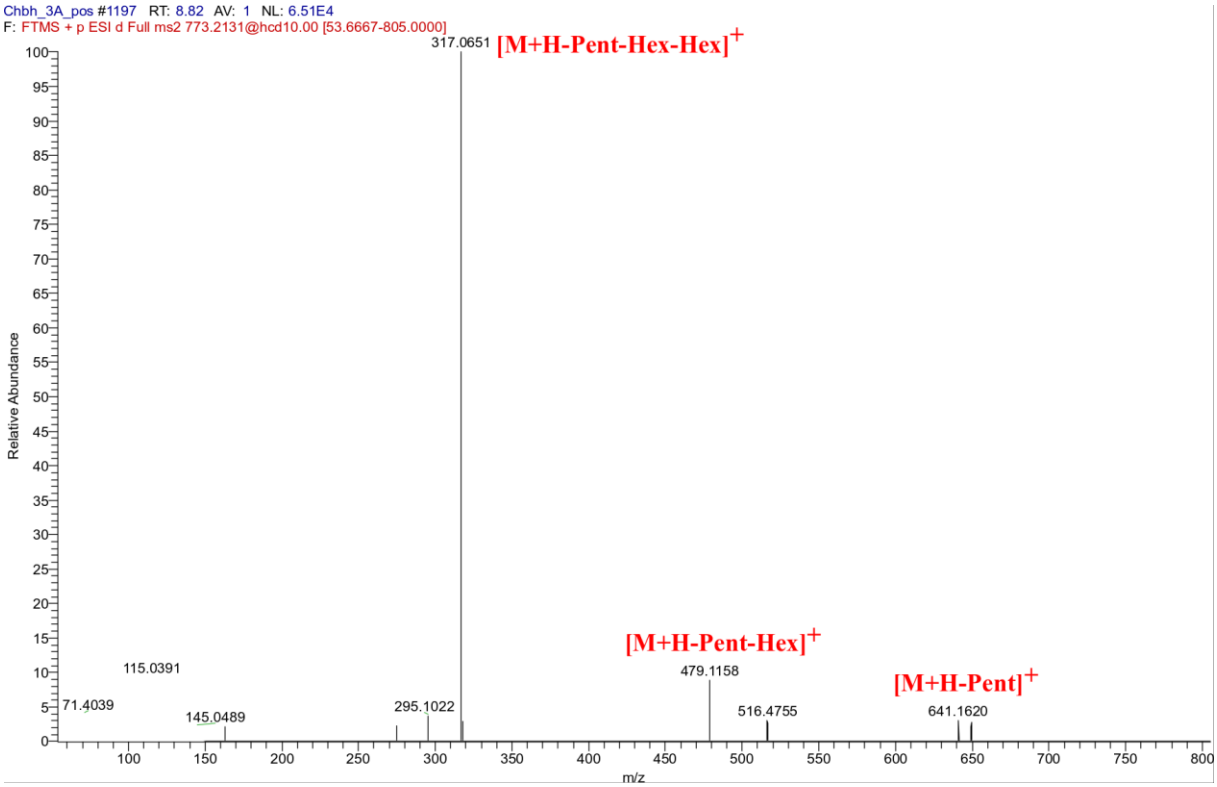

Figure S5: MS^2 spectrum of Compound **3**

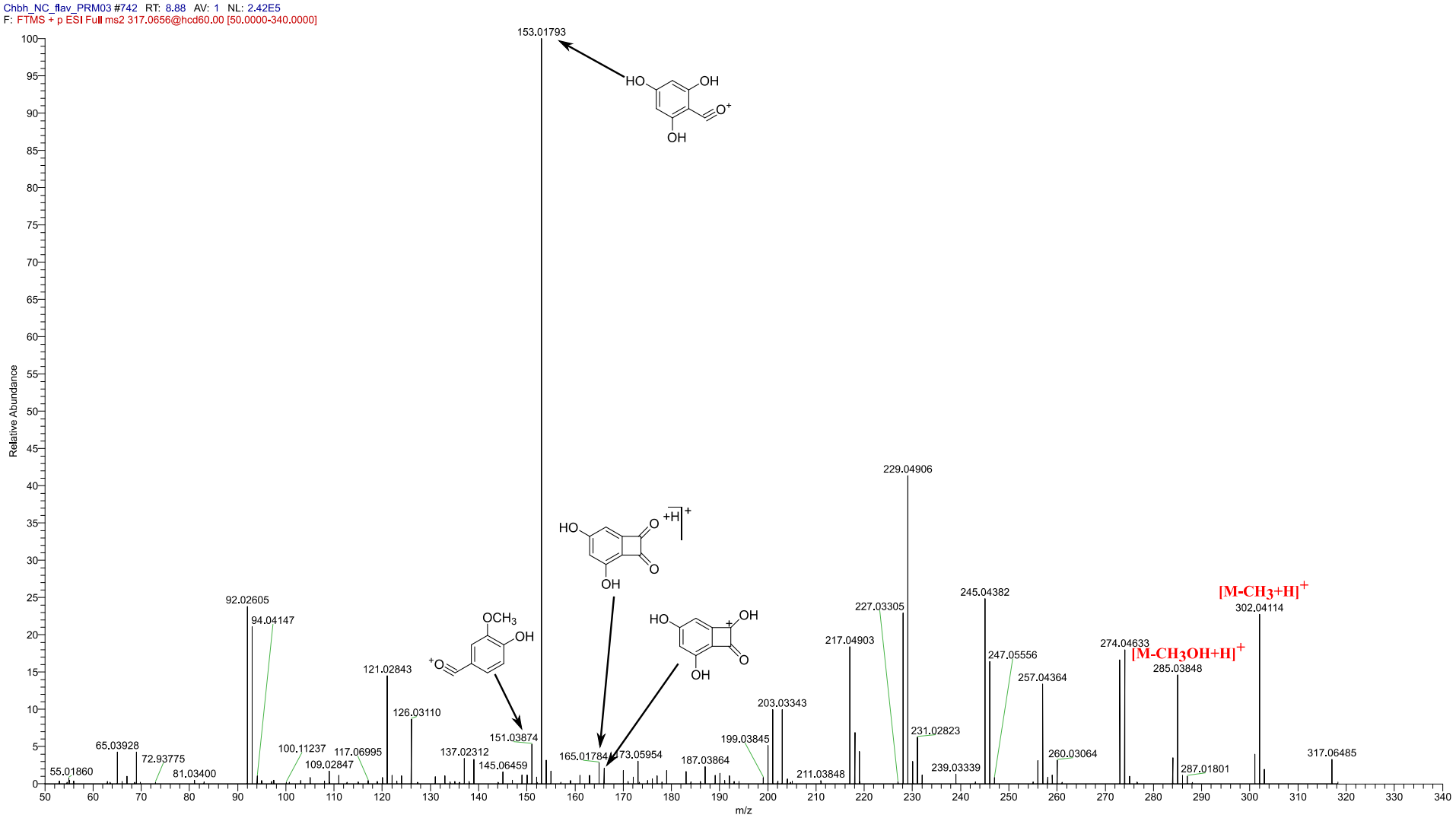

Figure S6: Pseudo MS^3 spectrum of precursor at *m/z* 317.0656 due to aglycone of compound **3**

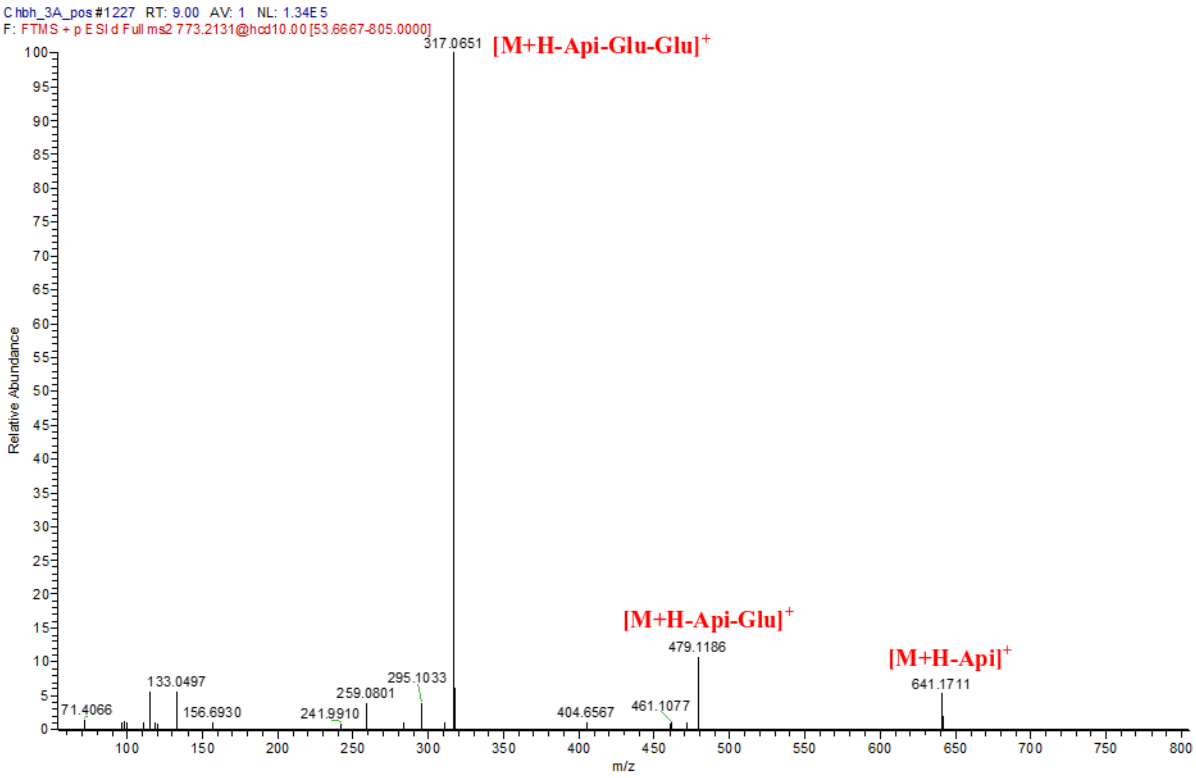

Figure S7: MS^2 spectrum of Compound **4**

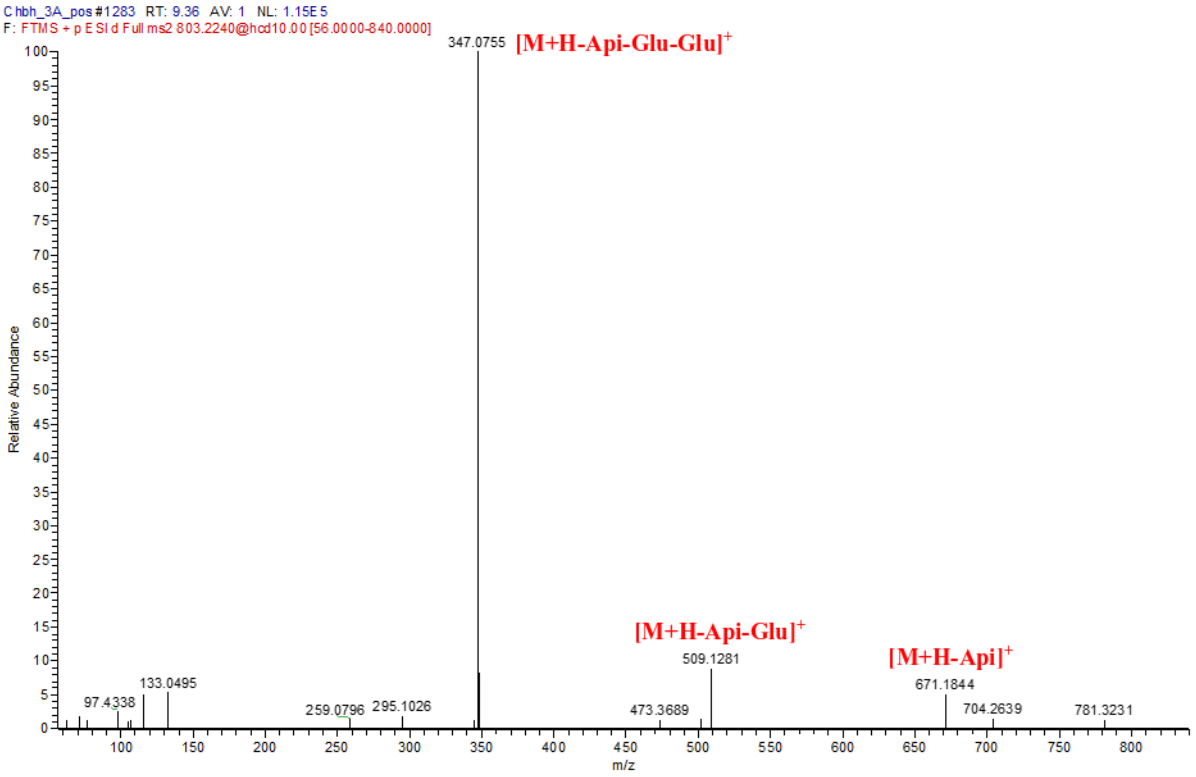

Figure S8: MS^2 spectrum of Compound **5**

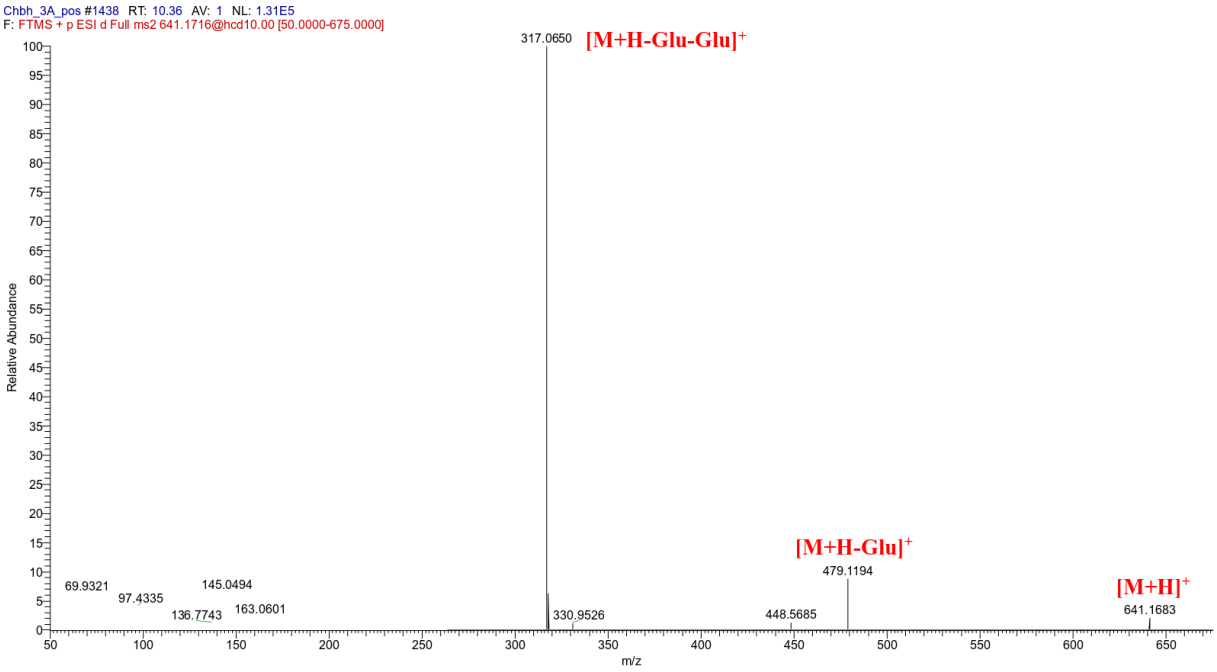

Figure S9: MS^2 spectrum of Compound **6**

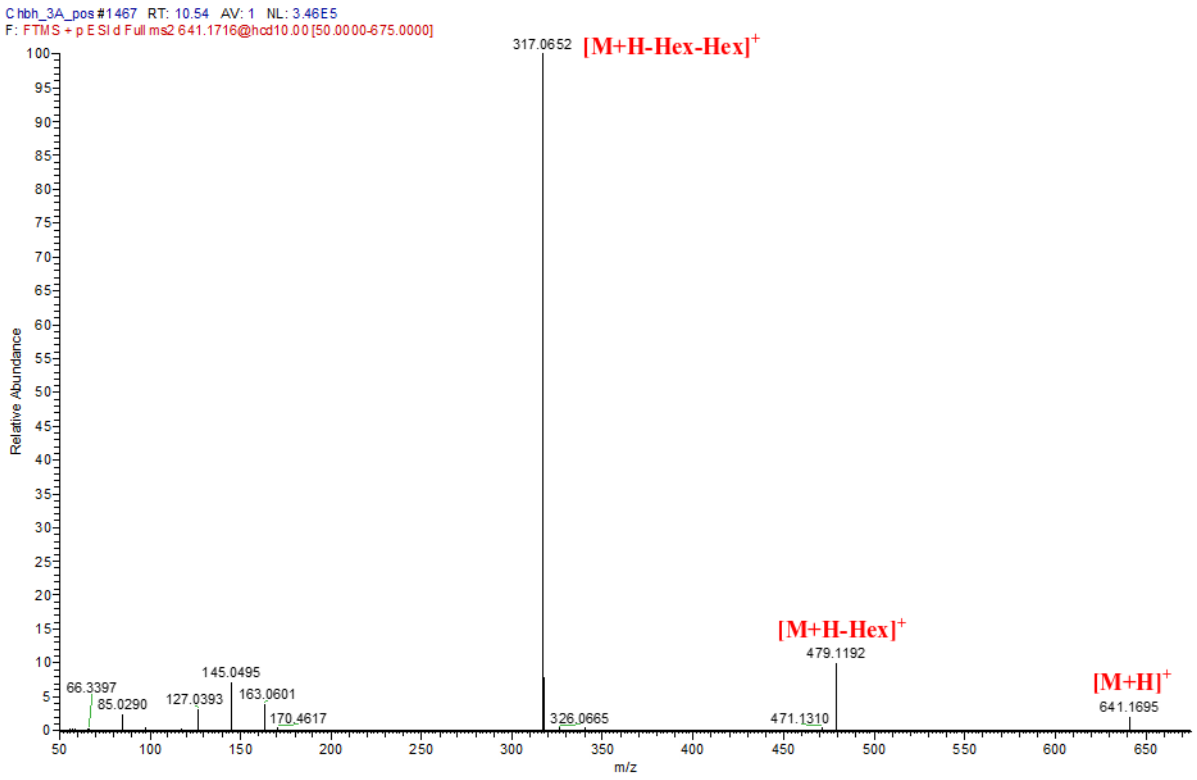

Figure S10: MS^2 spectrum of Compound **7**

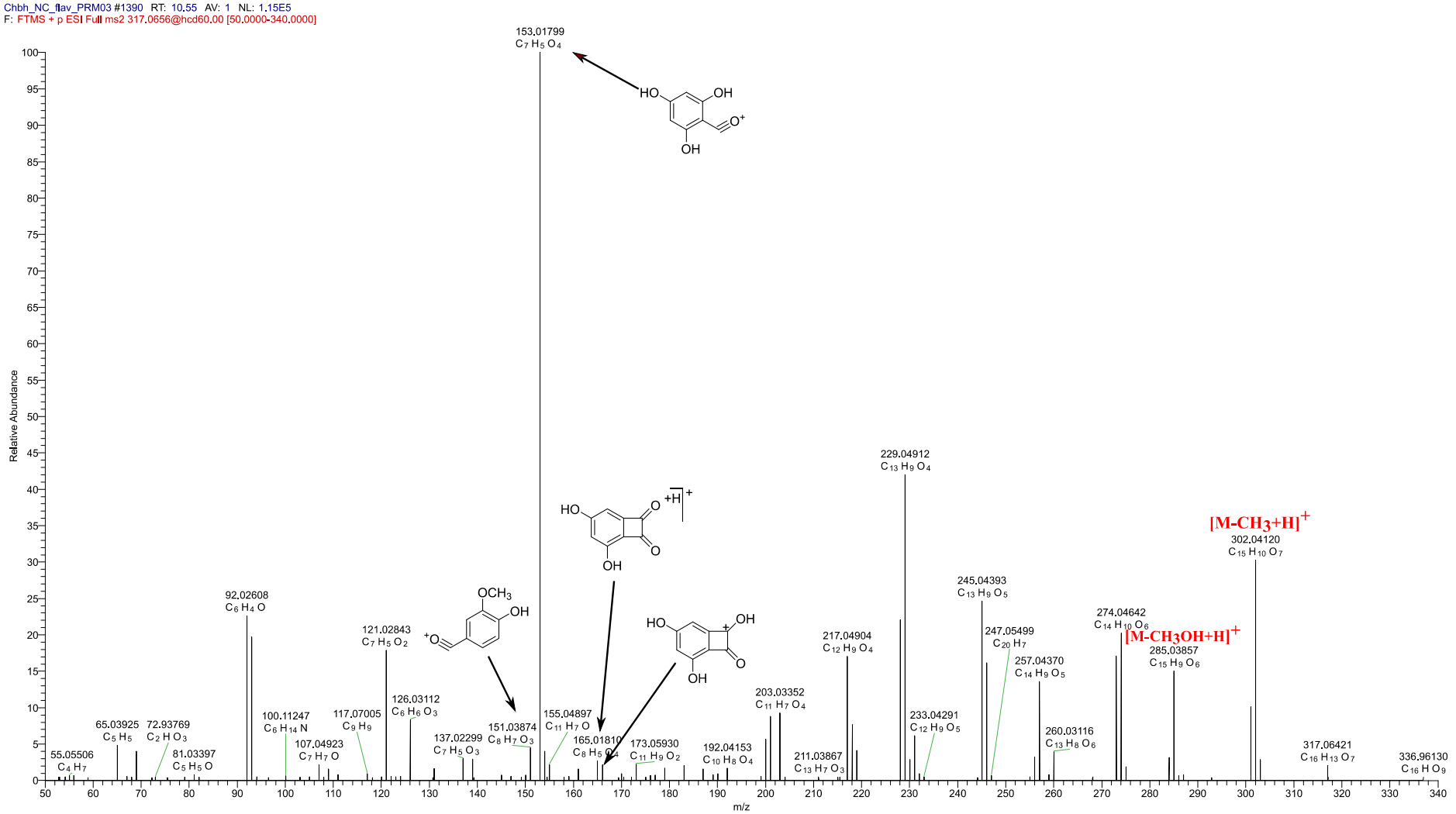

Figure S11: Pseudo MS^3 spectrum of precursor at *m/z* 317.0656 due to aglycone of compound **7**

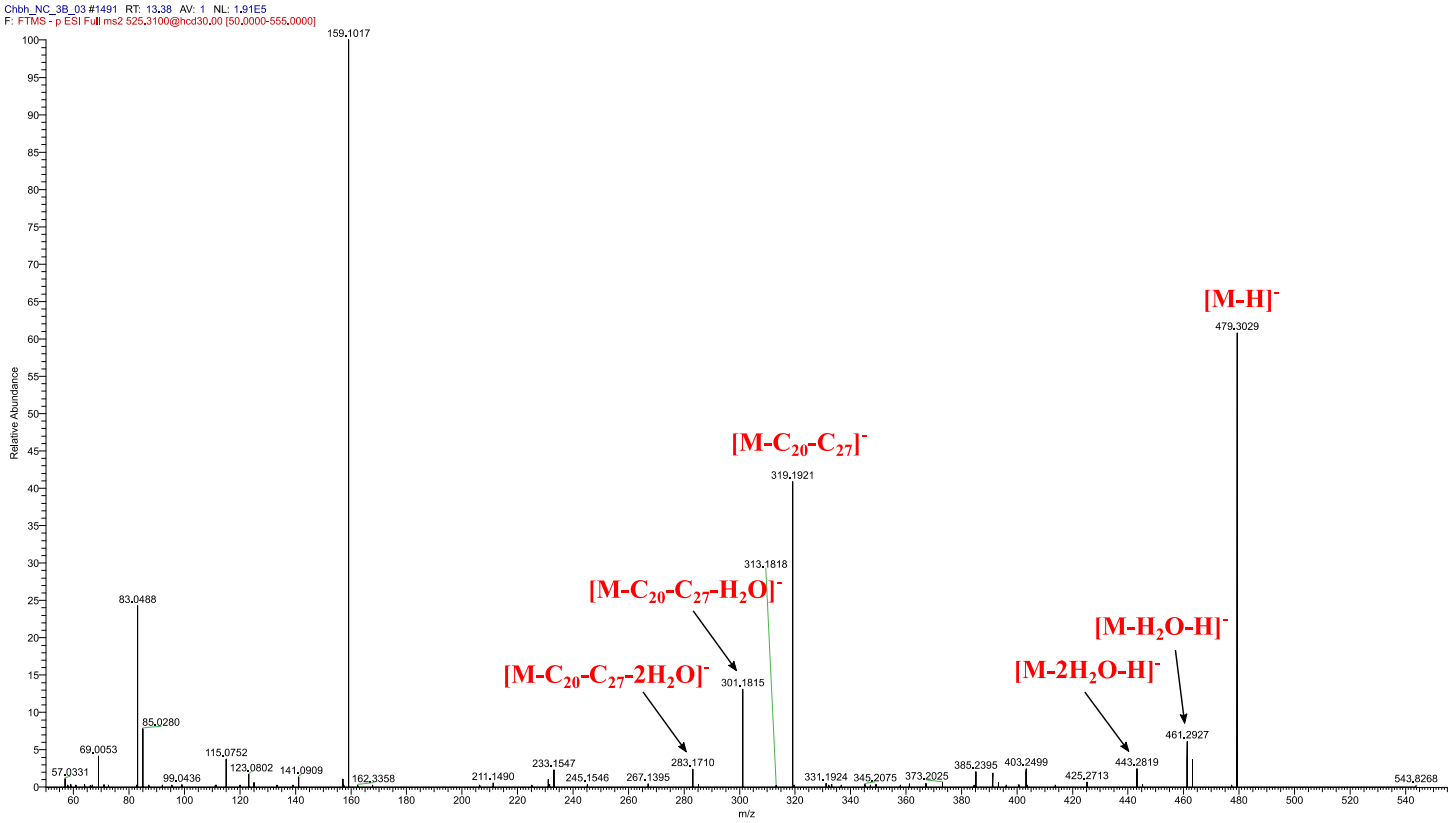

Figure S12: MS^2 spectrum of Compound **8**

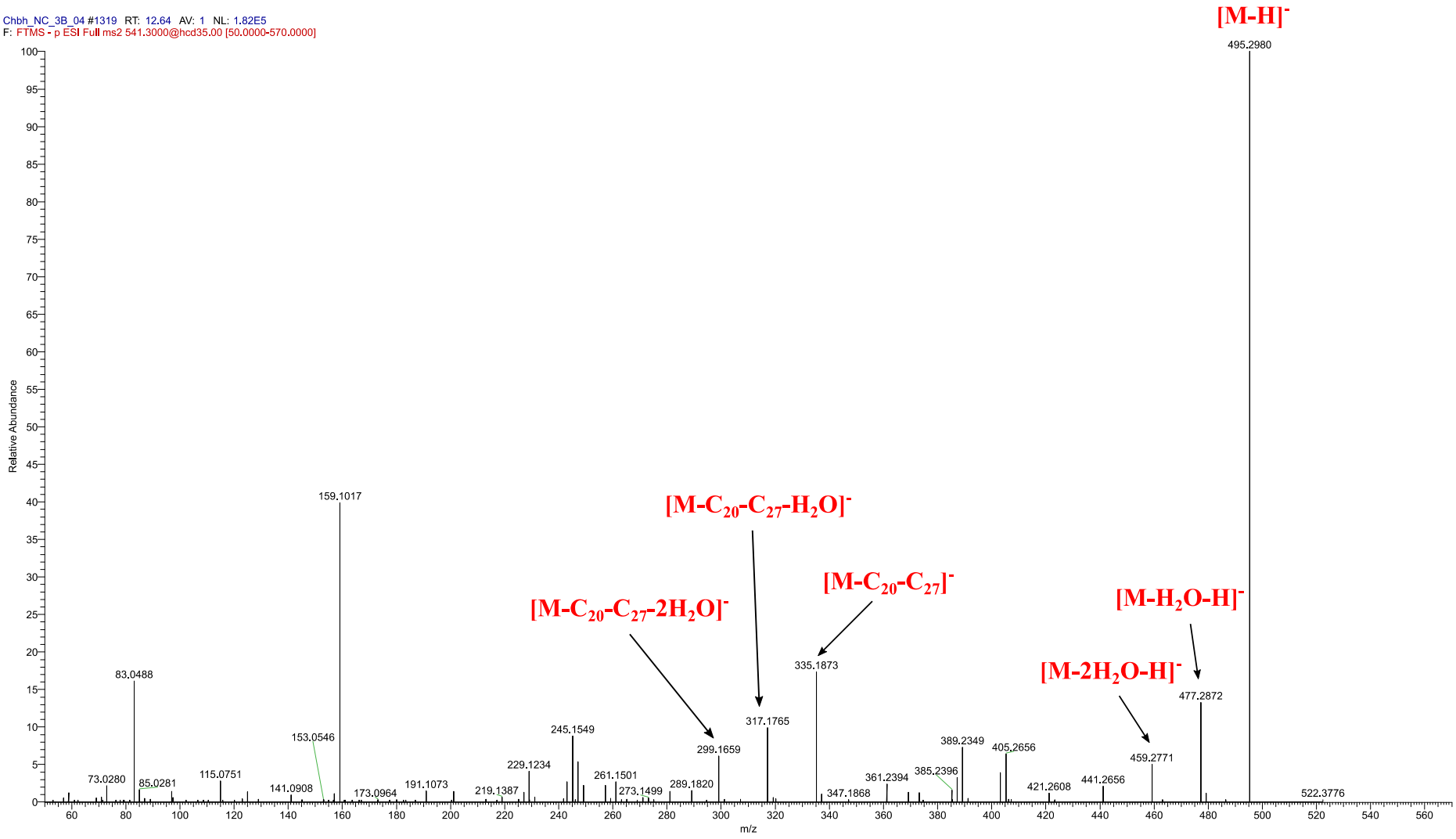

Figure S13: MS^2 spectrum of Compound **9**

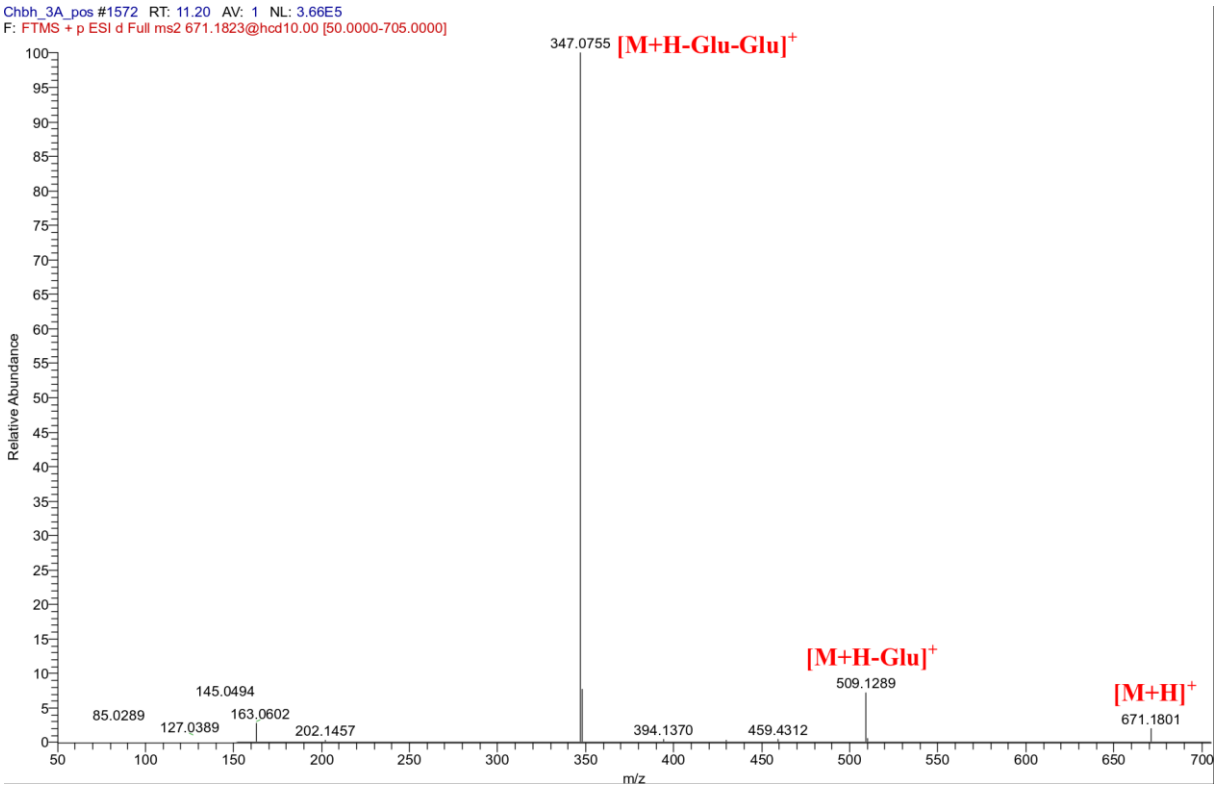

Figure S14: MS^2 spectrum of Compound **10**

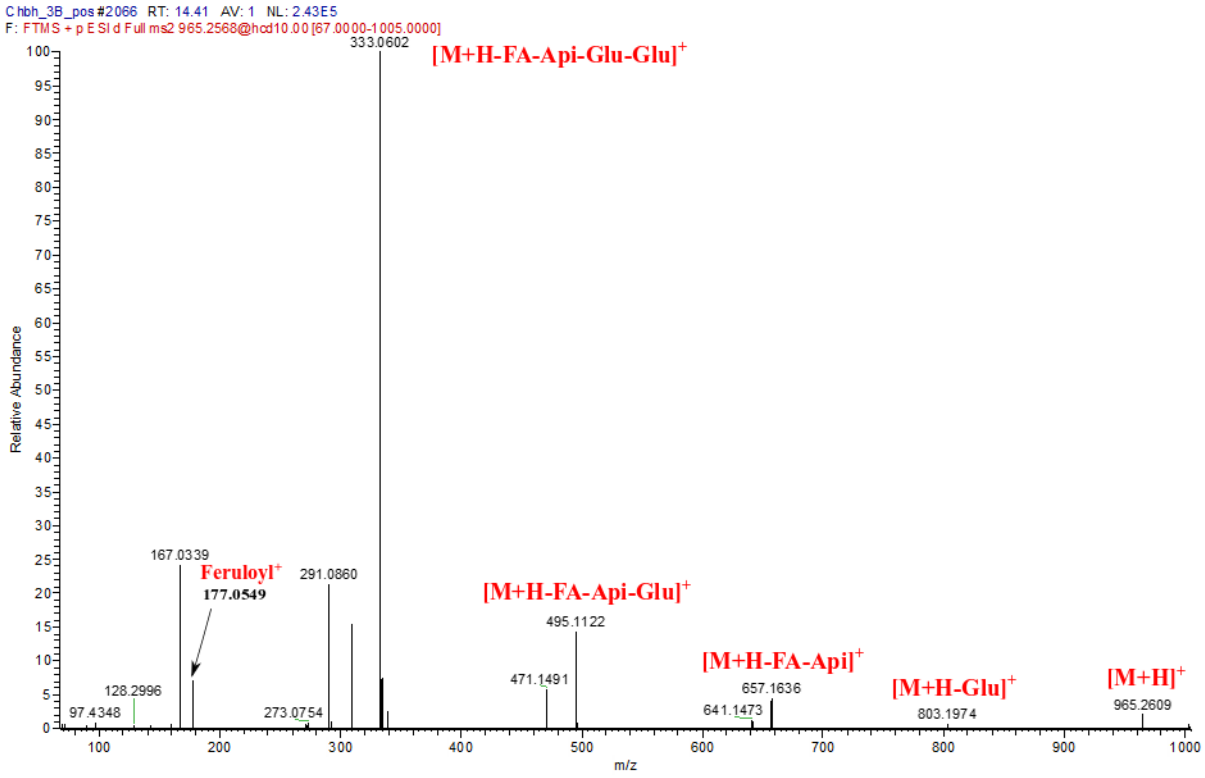

Figure S15: MS^2 spectrum of Compound **11**

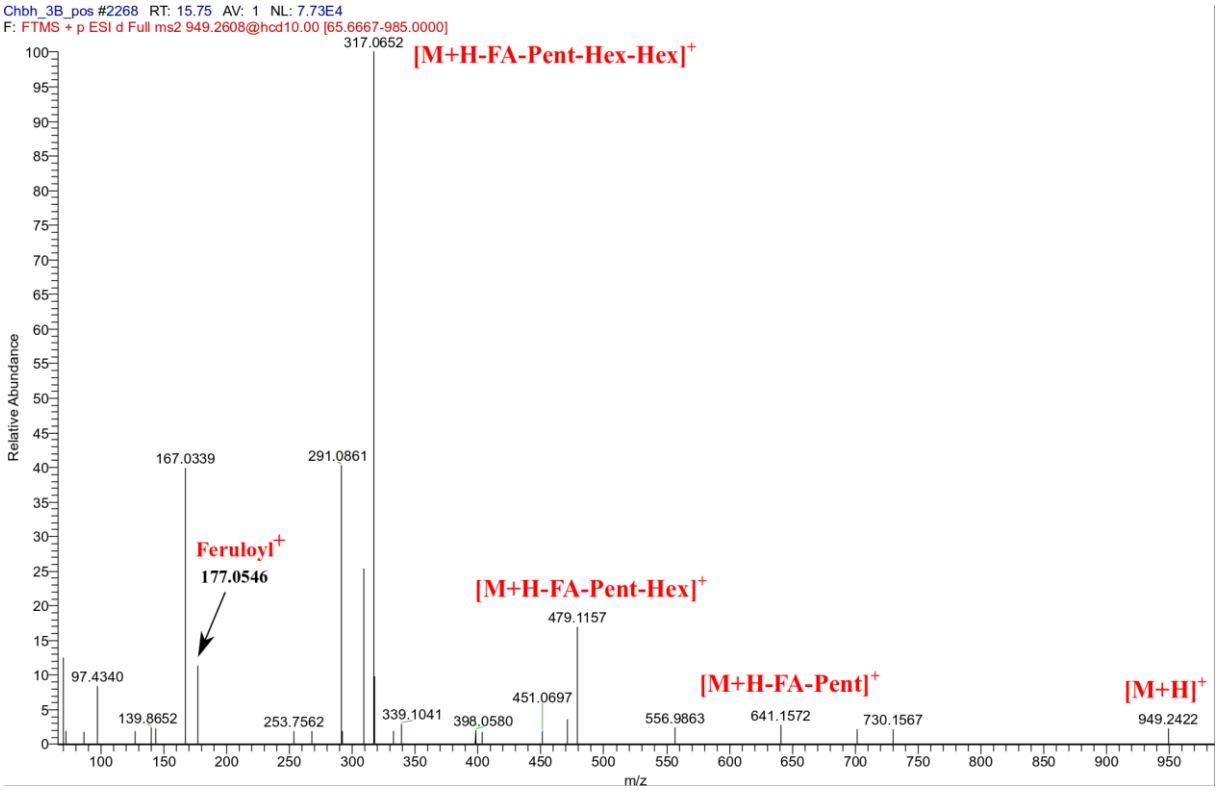

Figure S16: MS^2 spectrum of Compound **12**

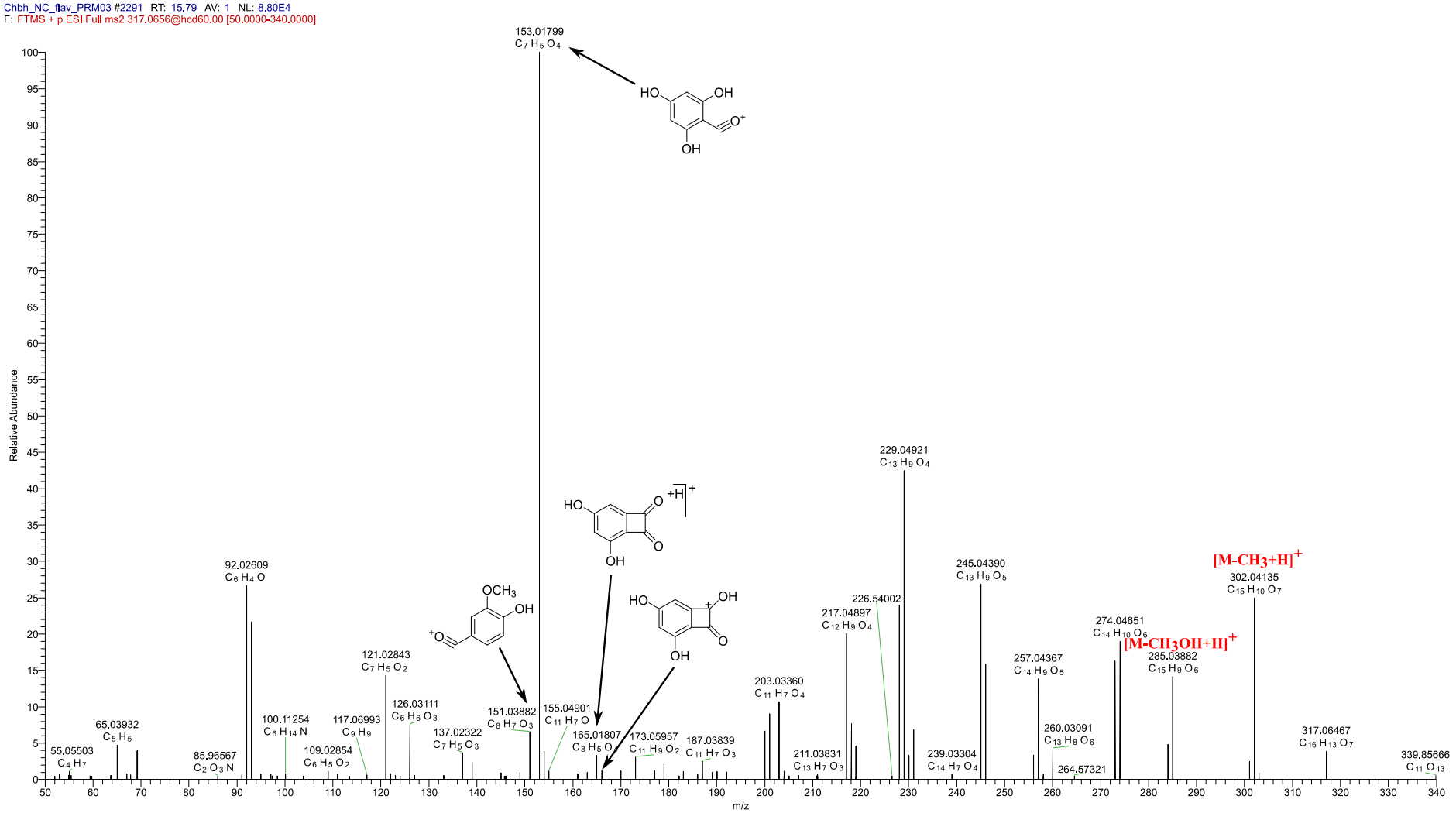

Figure S17: Pseudo MS^3 spectrum of precursor at *m/z* 317.0656 due to aglycone of compound **12**

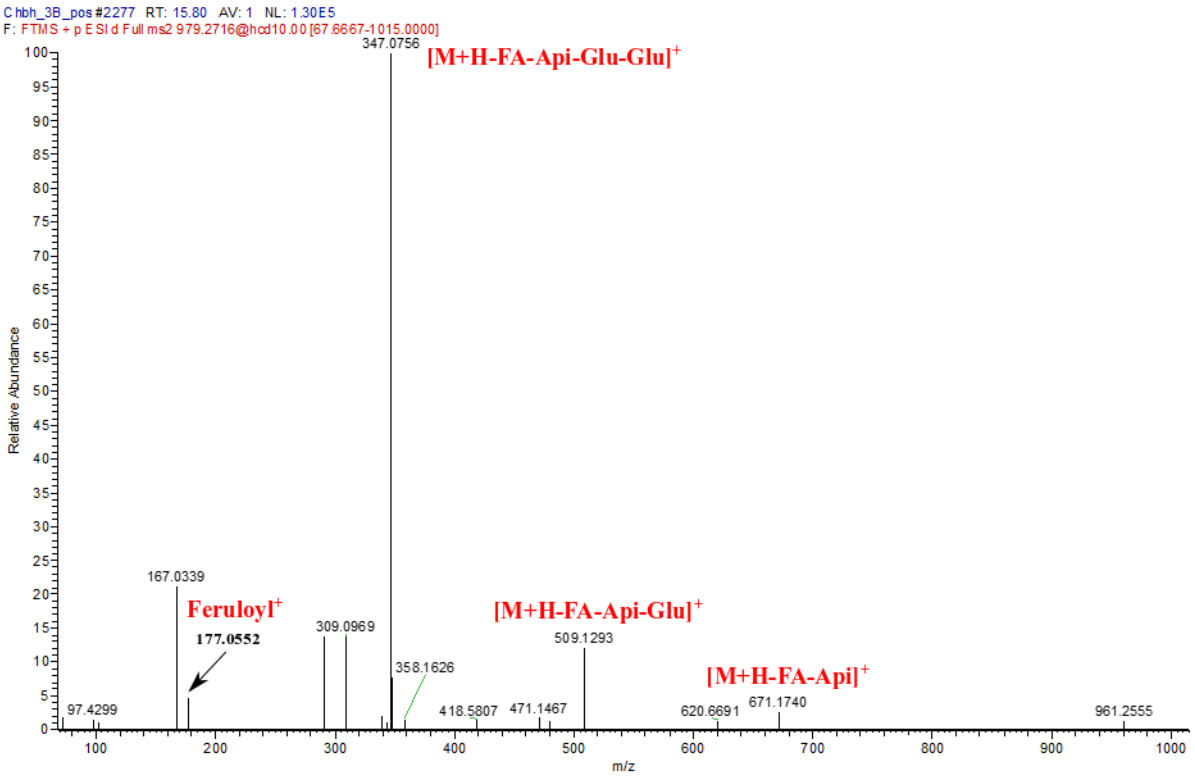

Figure S18: MS^2 spectrum of Compound **13**

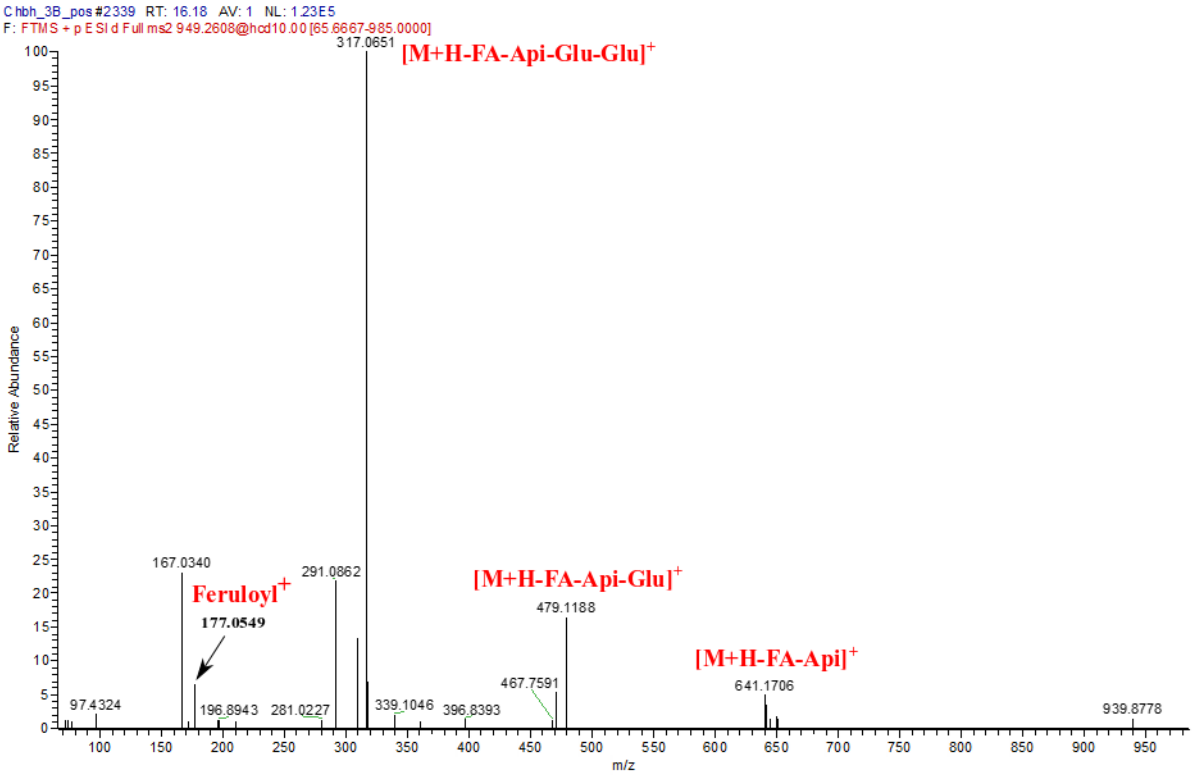

Figure S19: MS^2 spectrum of Compound **14**

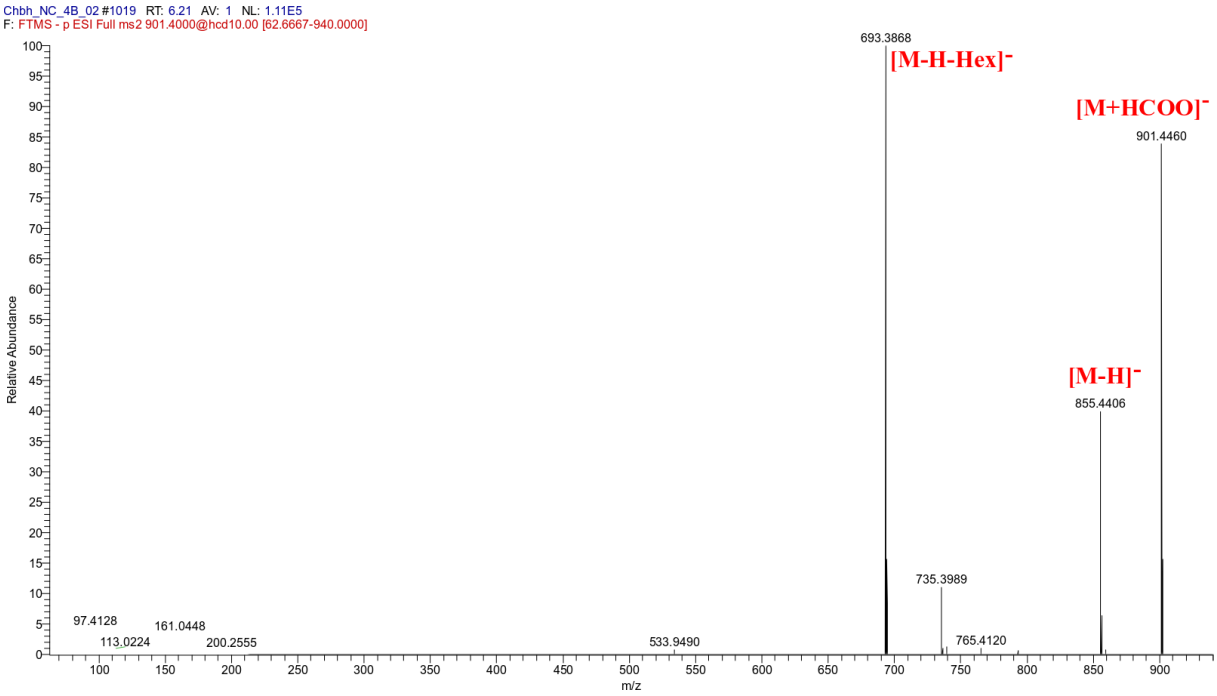

Figure S20: MS^2 spectrum (NCE=10) of Compound **15**

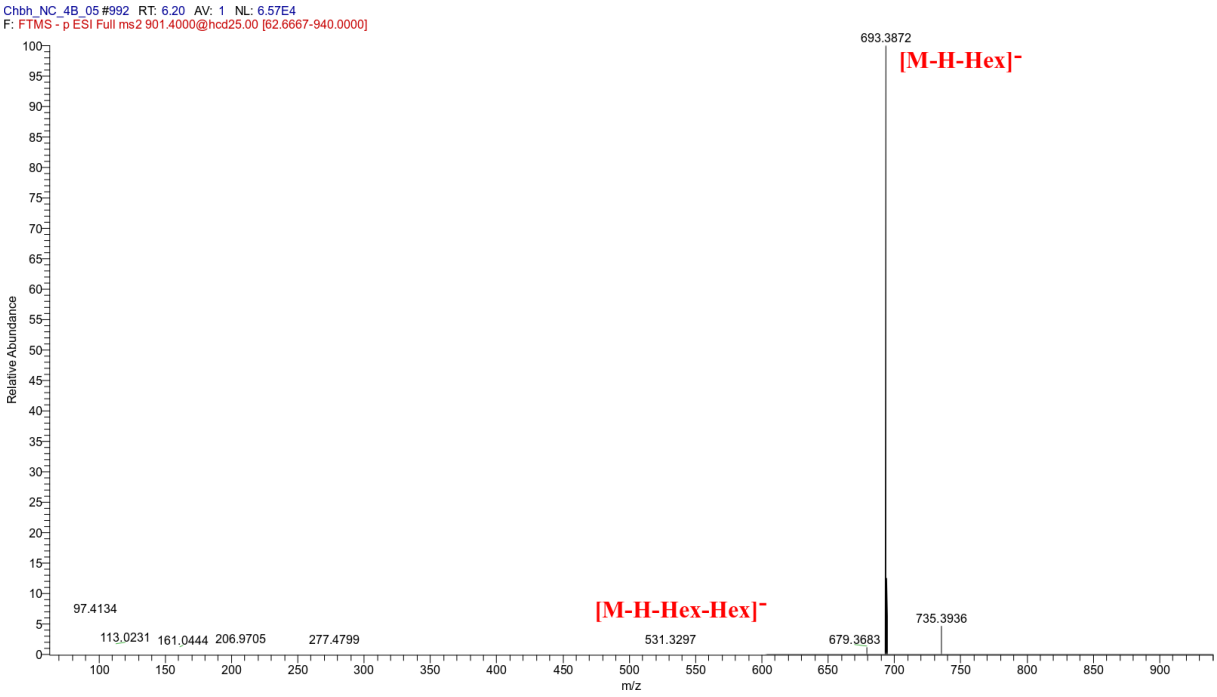

Figure S21: MS^2 spectrum (NCE=25) of Compound **15**

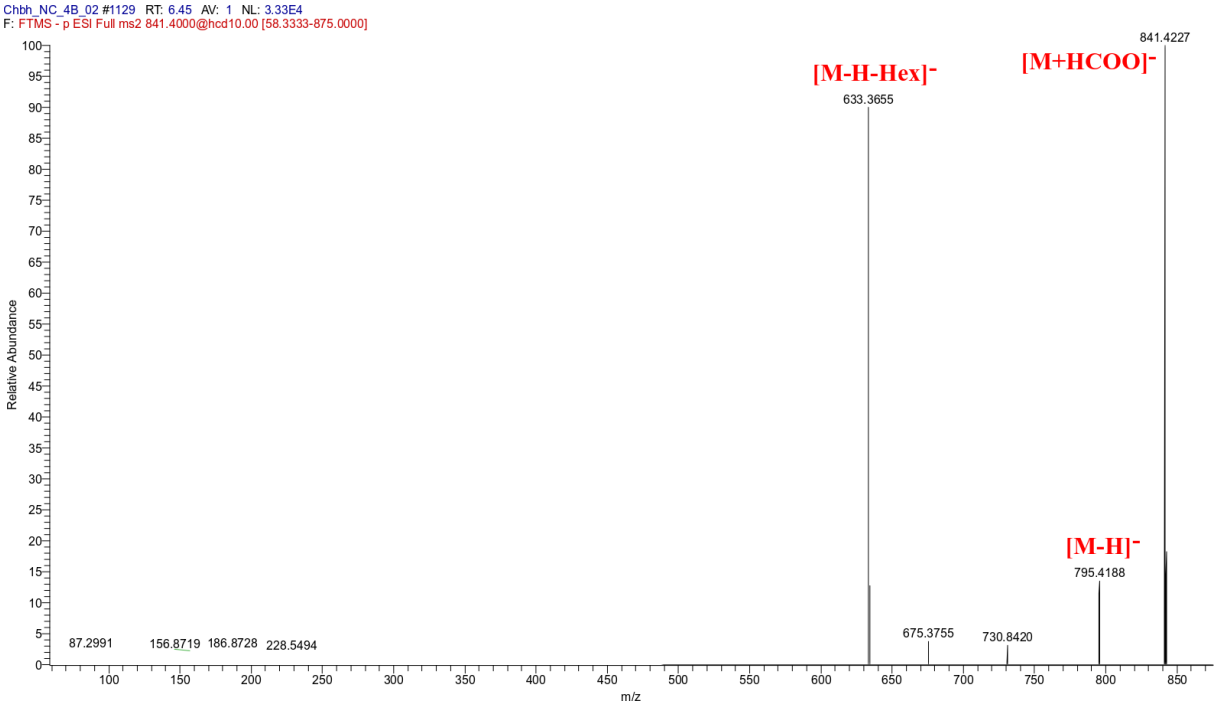

Figure S22: MS^2 spectrum (NCE=10) of Compound **16**

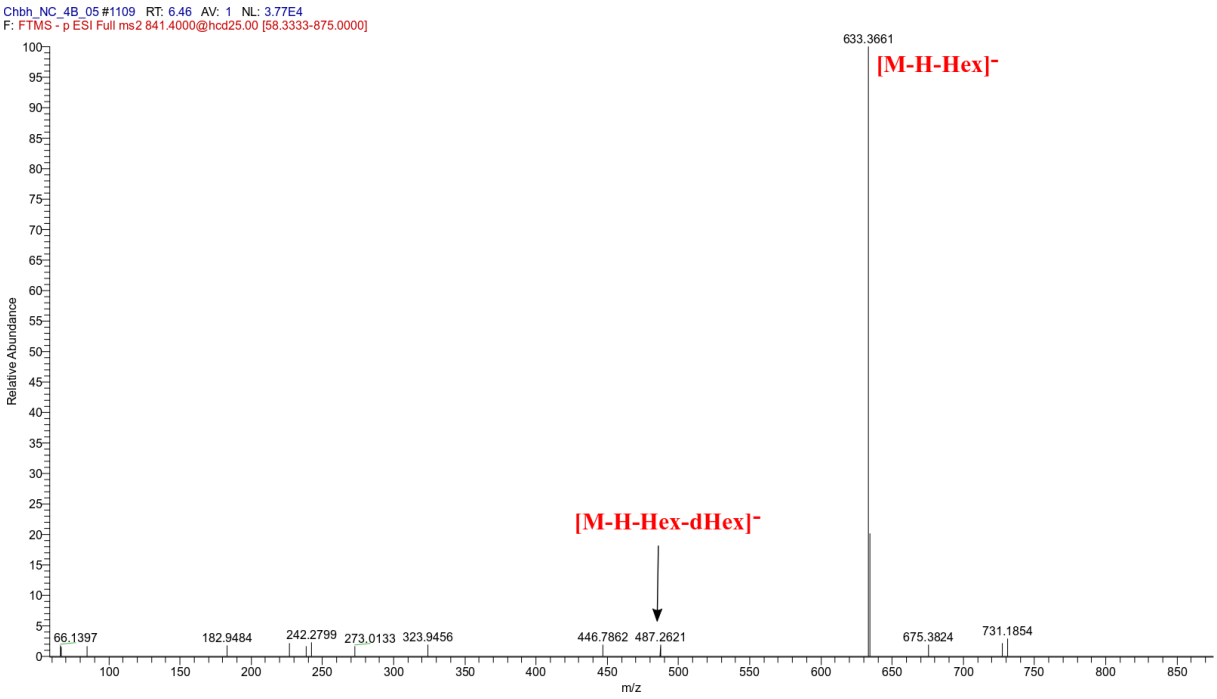

Figure S23: MS^2 spectrum (NCE=25) of Compound **16**

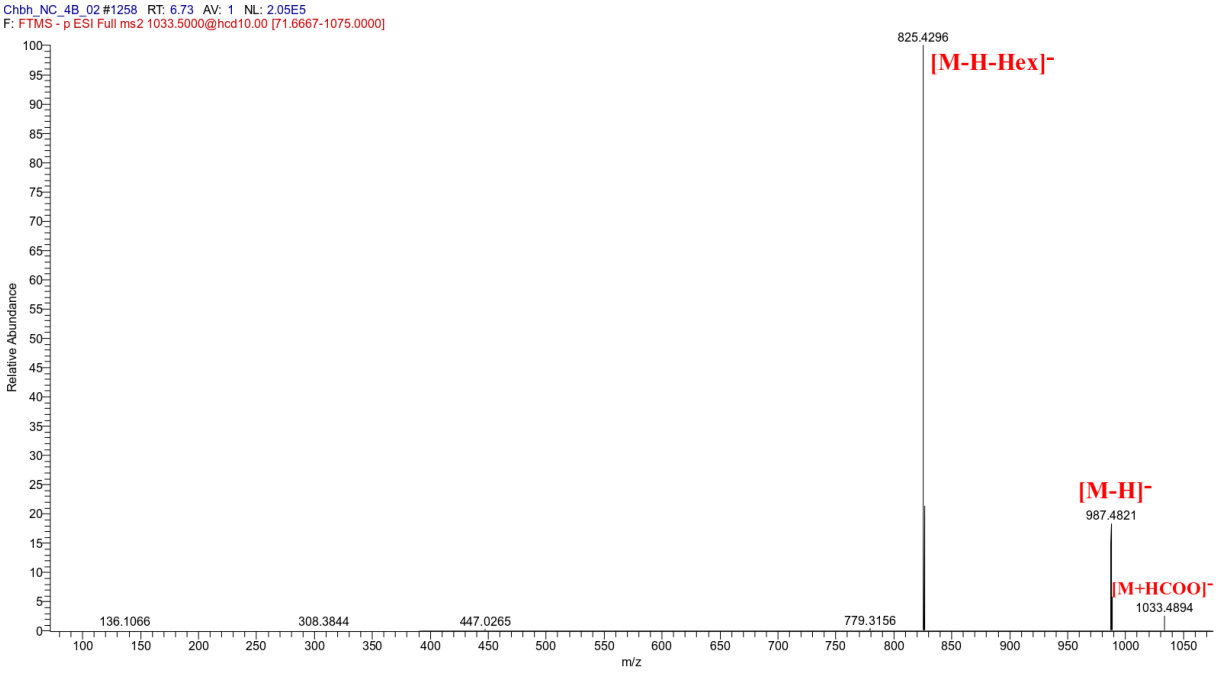

Figure S24: MS^2 spectrum (NCE=10) of Compound **17**

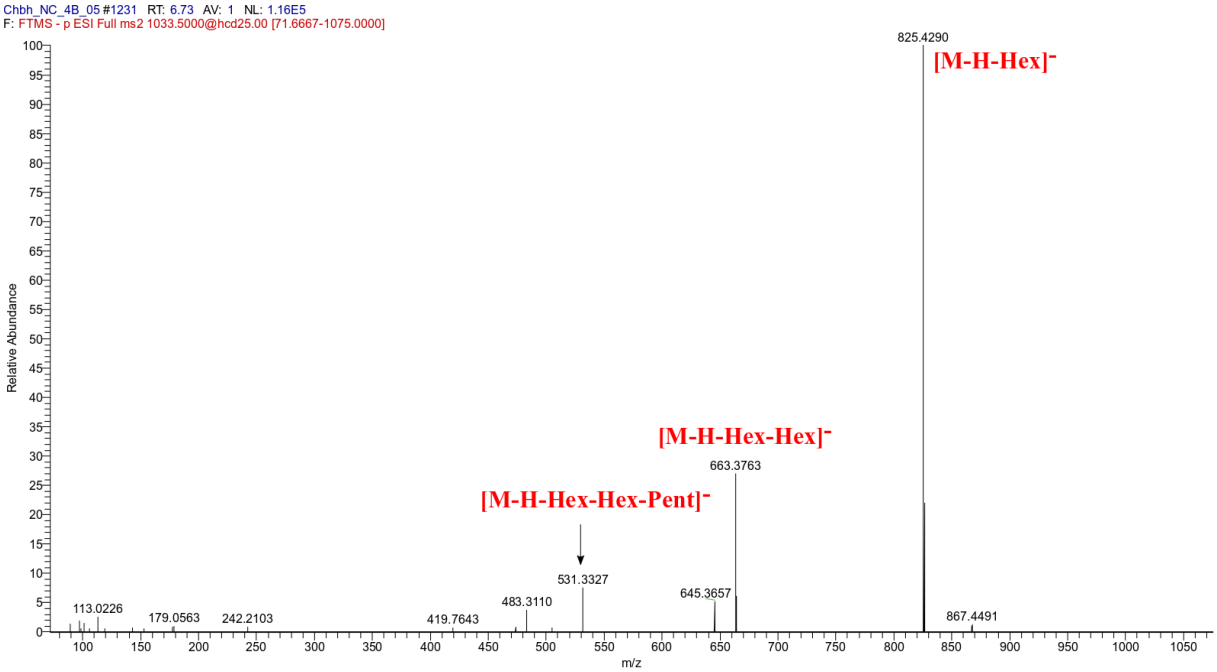

Figure S25: MS^2 spectrum (NCE=25) of Compound **17**

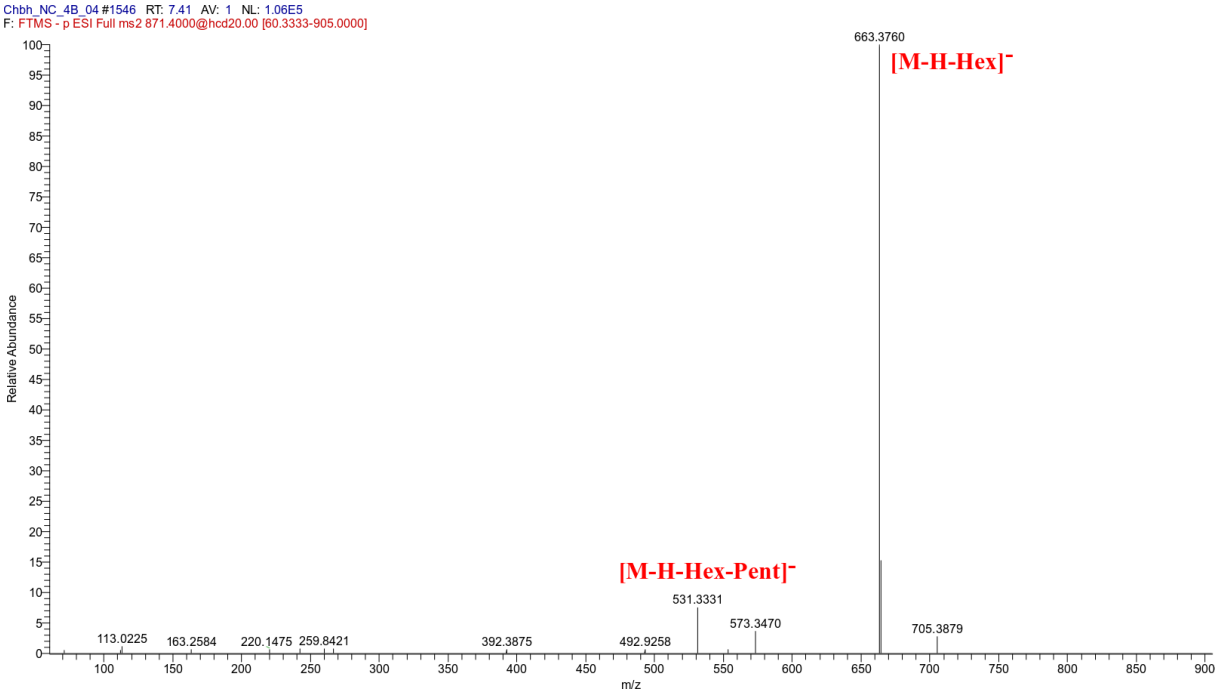

Figure S26: MS^2 spectrum of Compound **18**

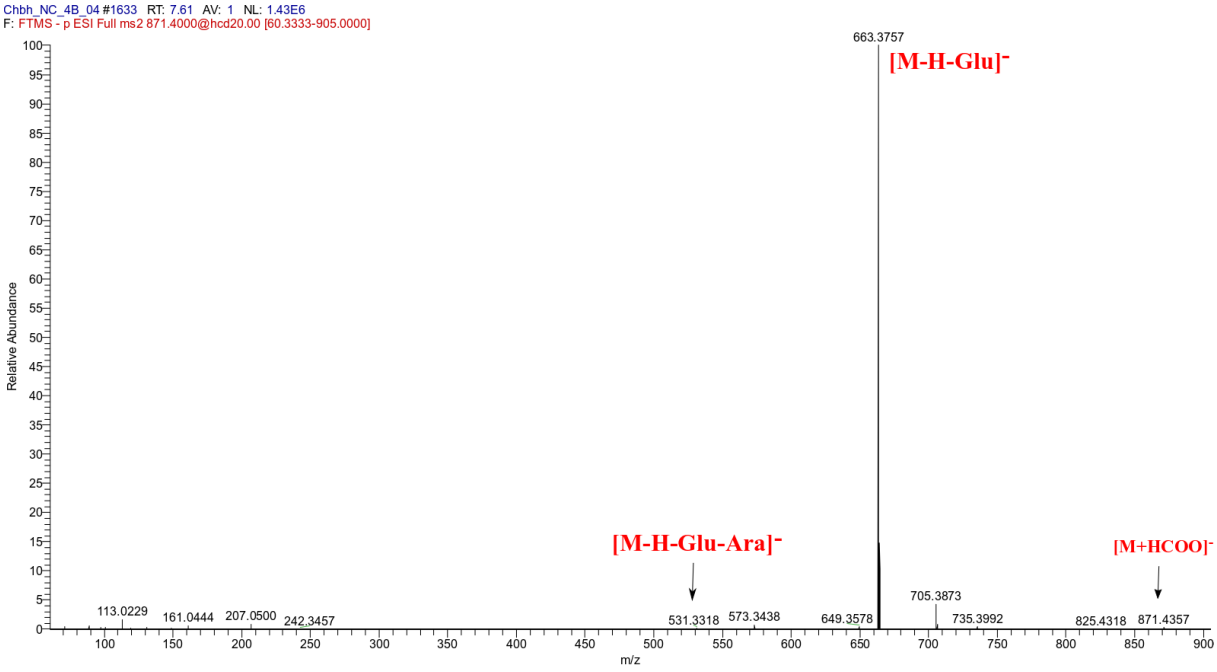

Figure S27: MS^2 spectrum of Compound **19**

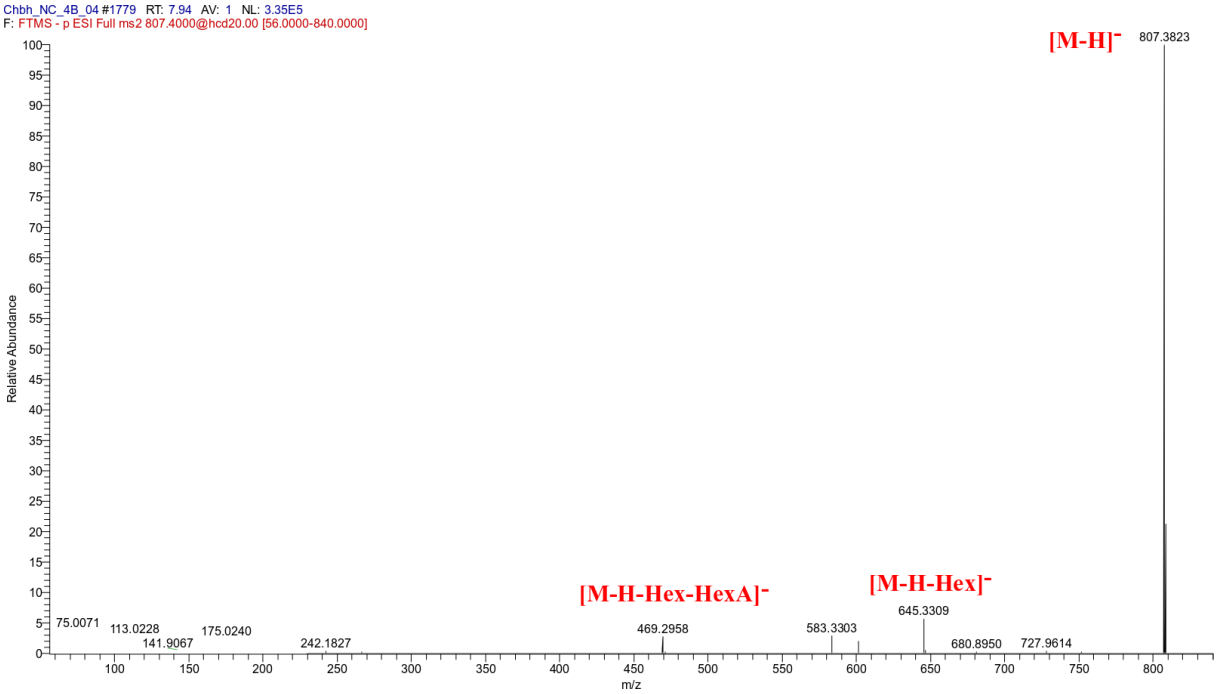

Figure S28: MS^2 spectrum of Compound **20**

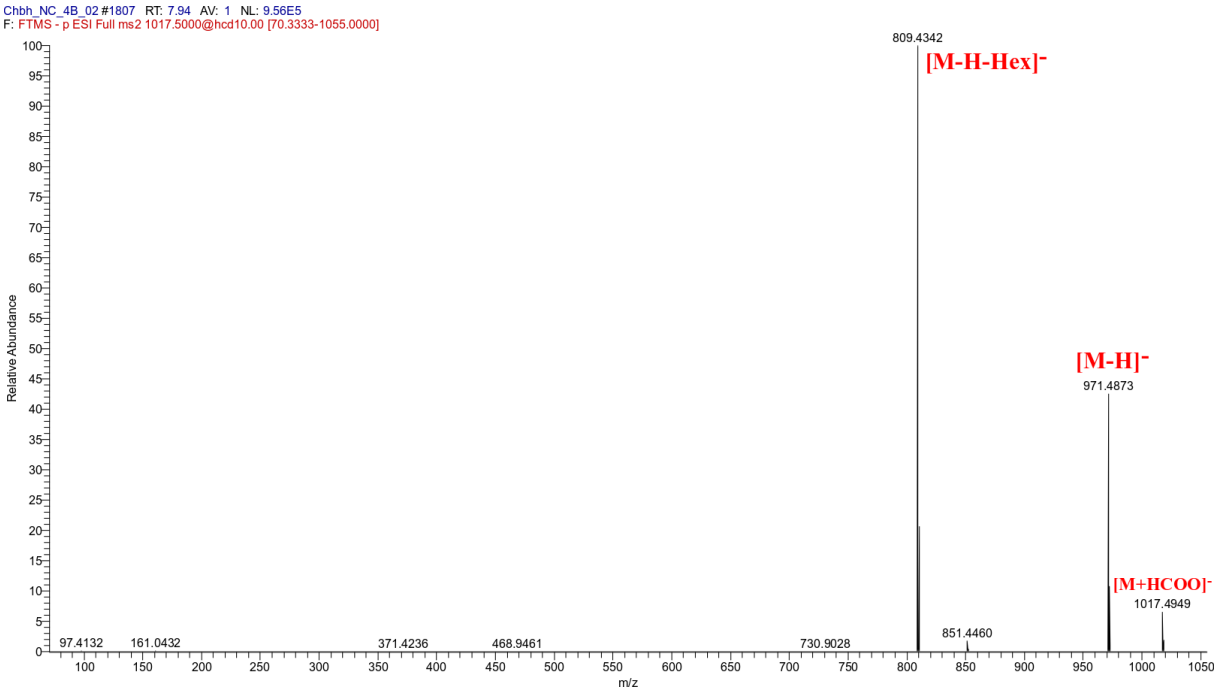

Figure S29: MS^2 spectrum (NCE=10) of Compound **21**

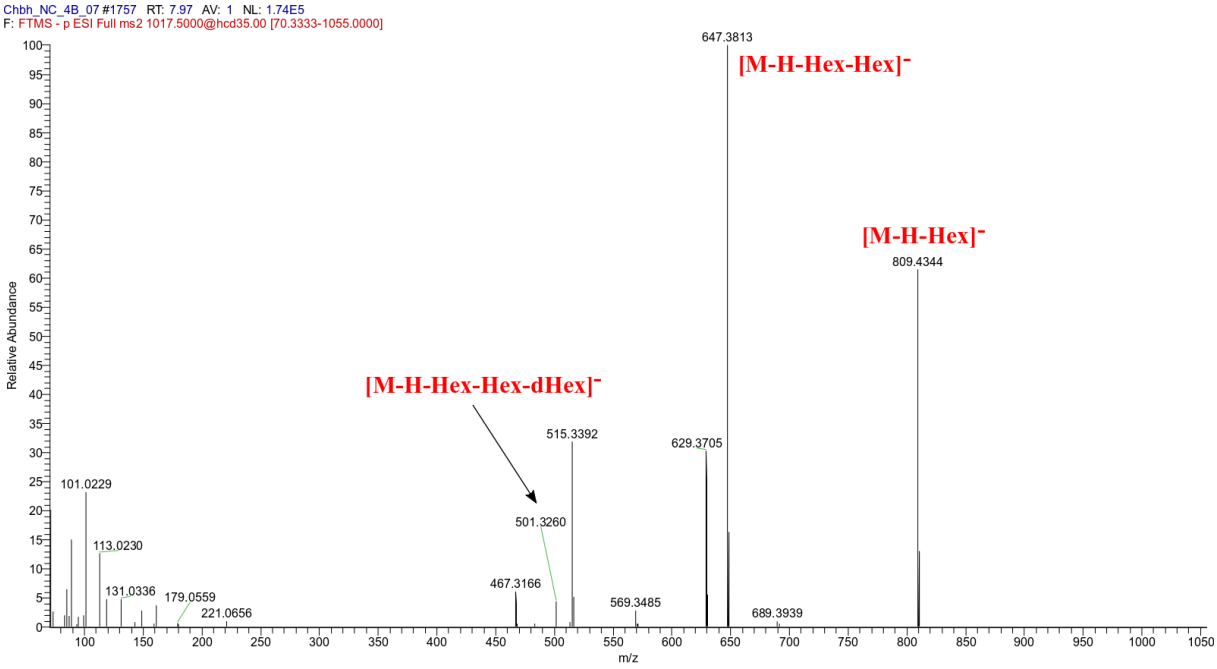

Figure S30: MS^2 spectrum (NCE=35) of Compound **21**

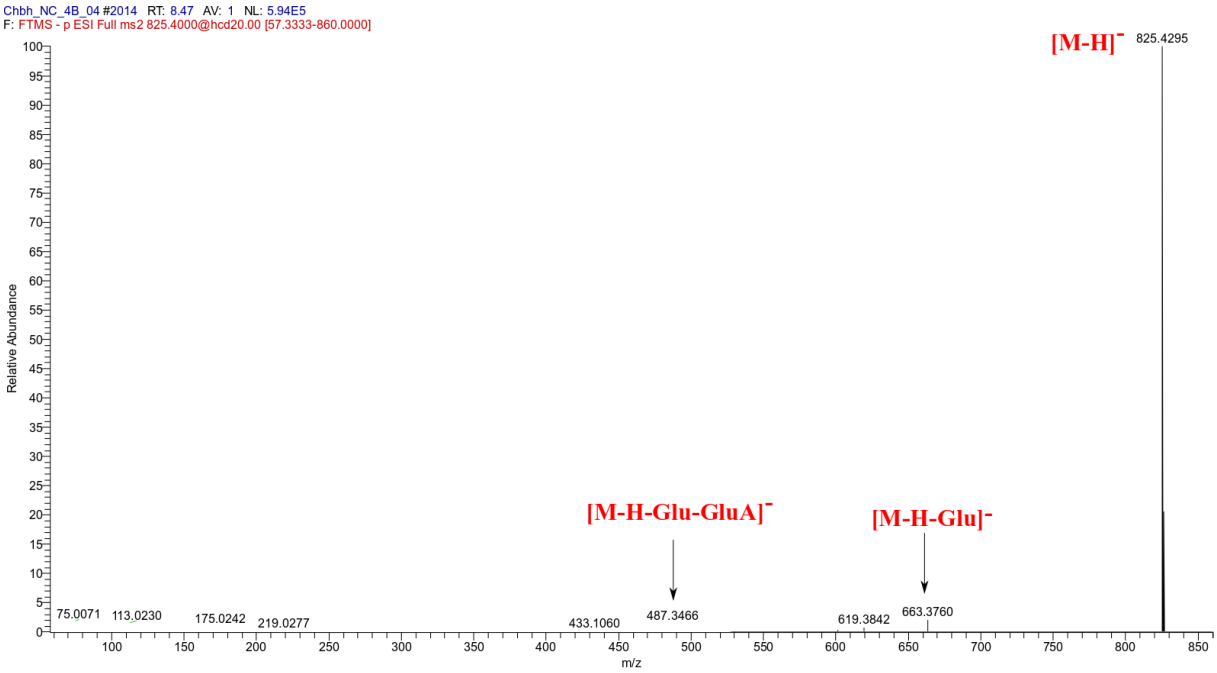

Figure S31: MS^2 spectrum of Compound **22**

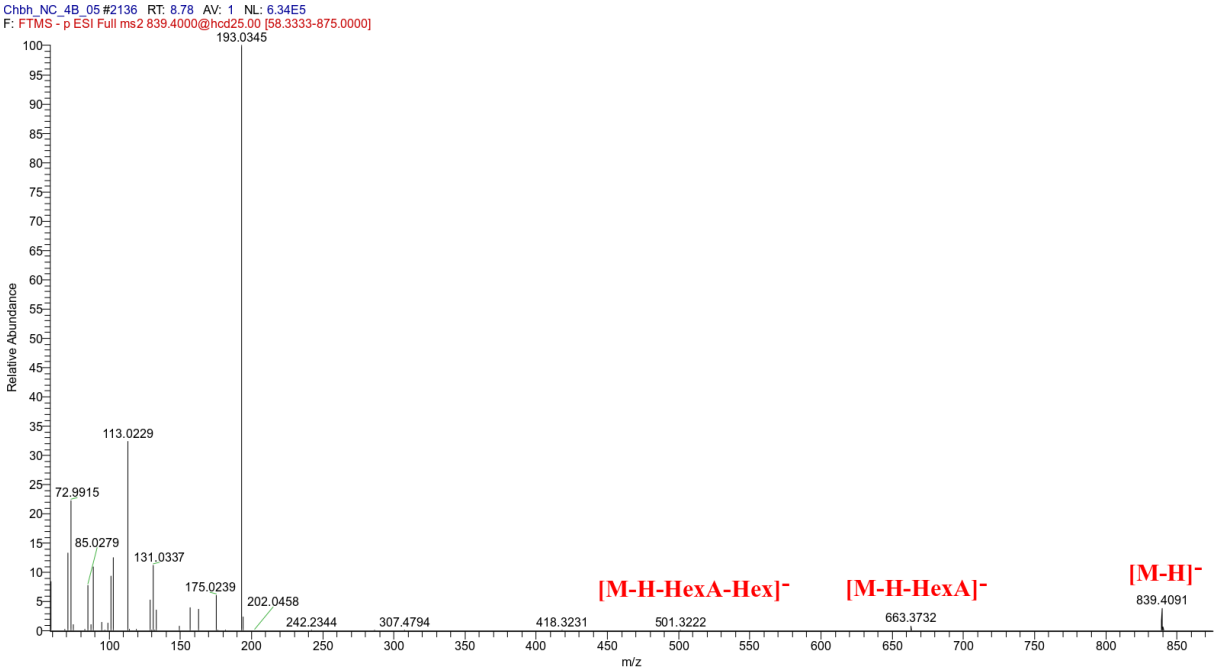

Figure S32: MS^2 spectrum of Compound **23**

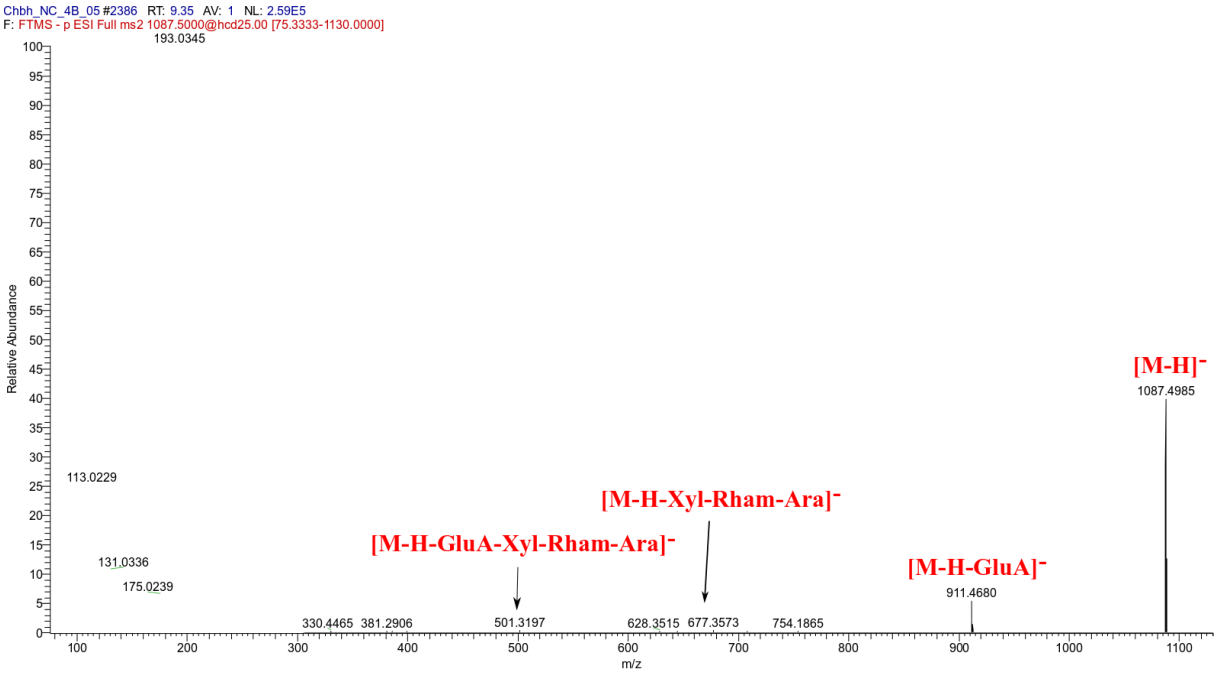

Figure S33: MS^2 spectrum of Compound **24**

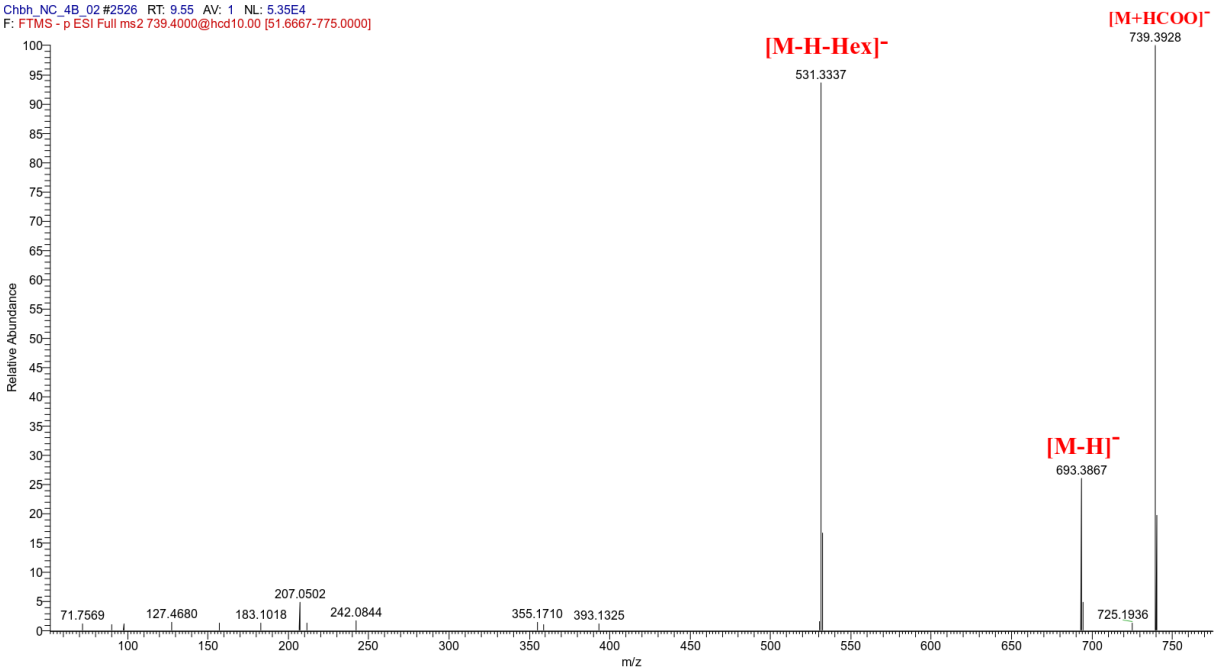

Figure S34: MS^2 spectrum of Compound **25**

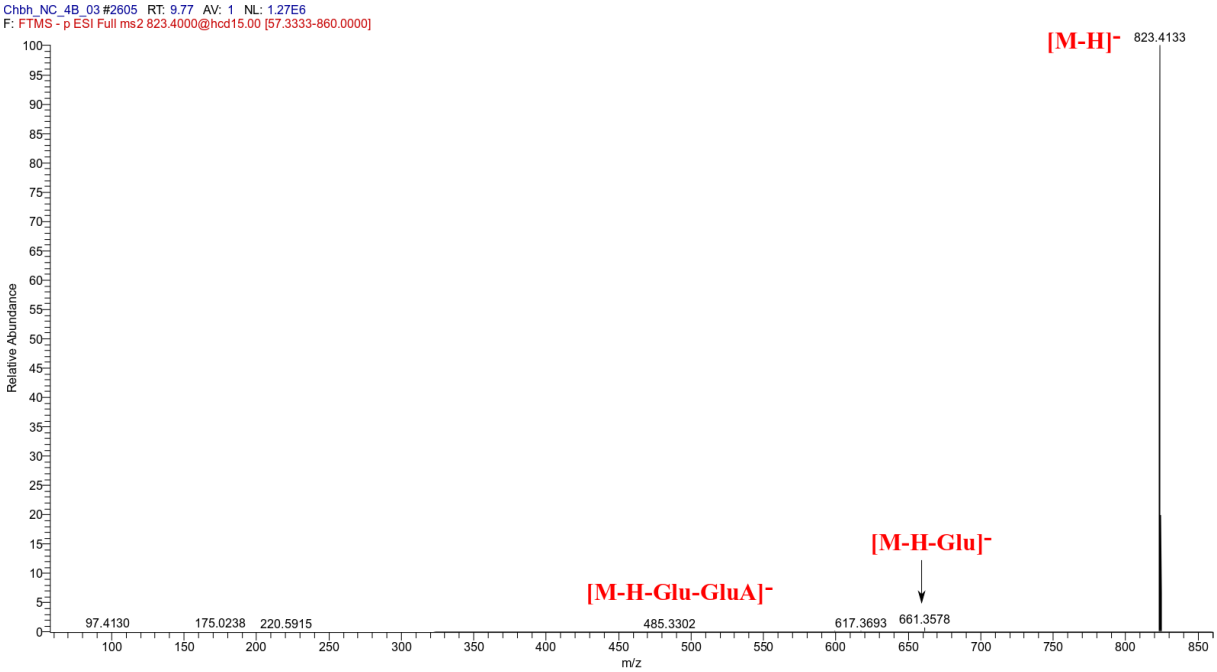

Figure S35: MS^2 spectrum of Compound **26**

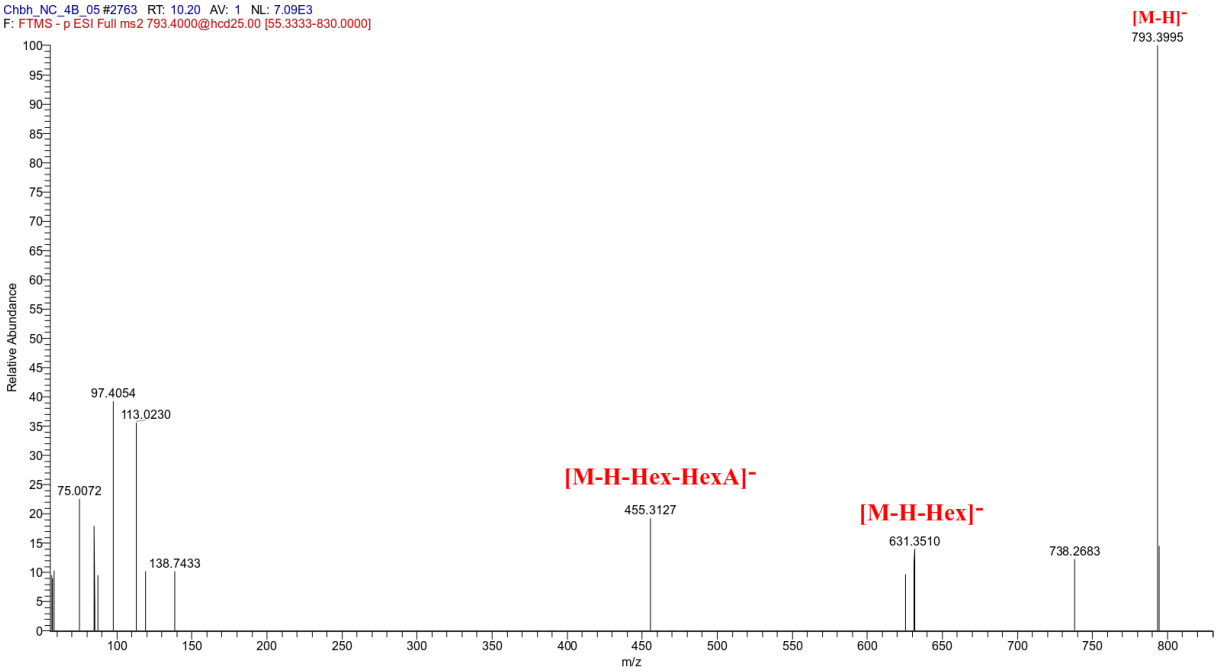

Figure S36: MS^2 spectrum of Compound **27**

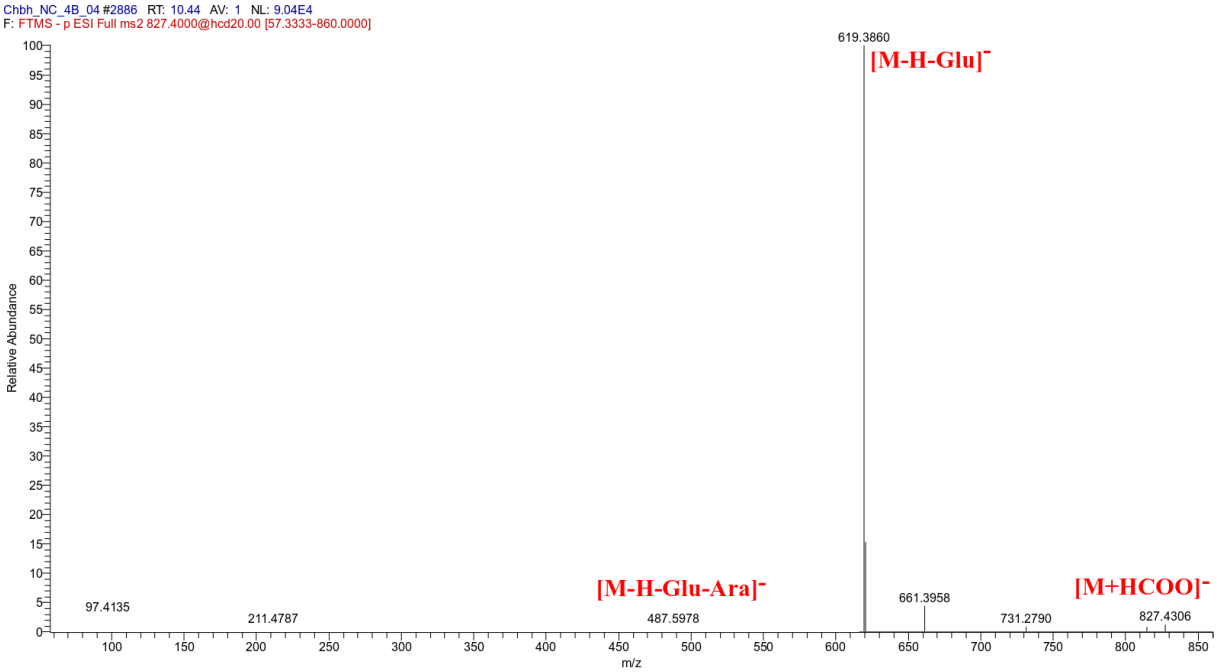

Figure S37: MS^2 spectrum of Compound **28**

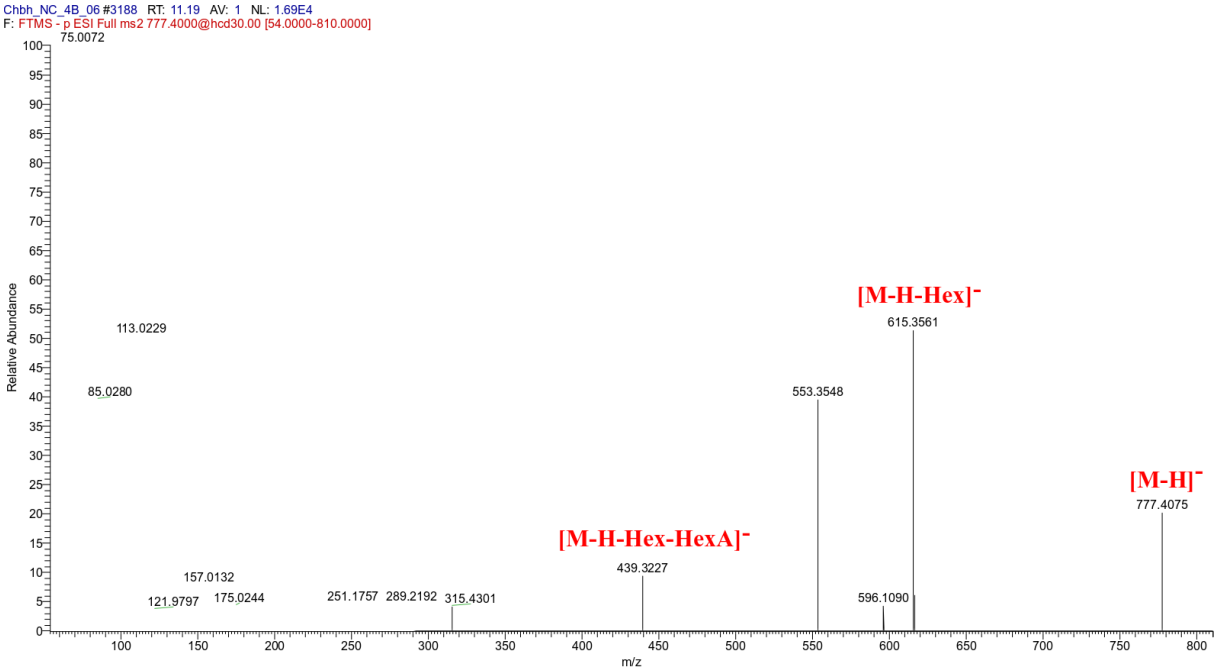

Figure S38: MS^2 spectrum of Compound **29**

Figure S39: MS^2 spectrum of Compound **30**

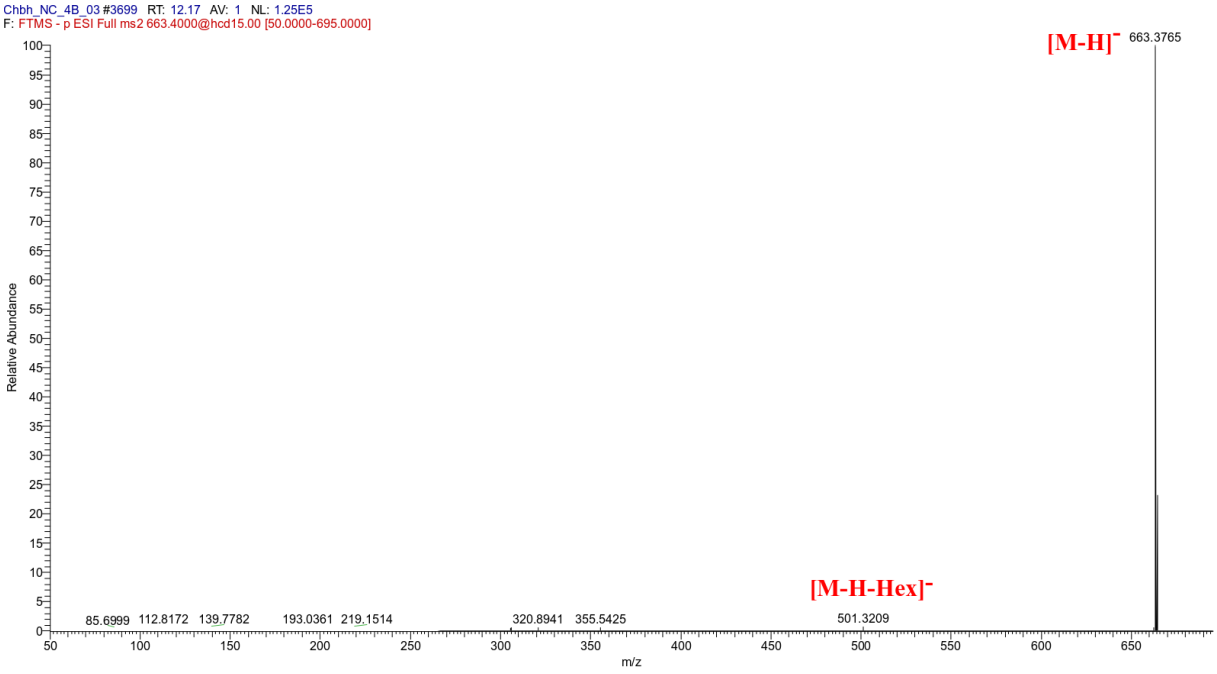

Figure S40: MS^2 spectrum of Compound **31**

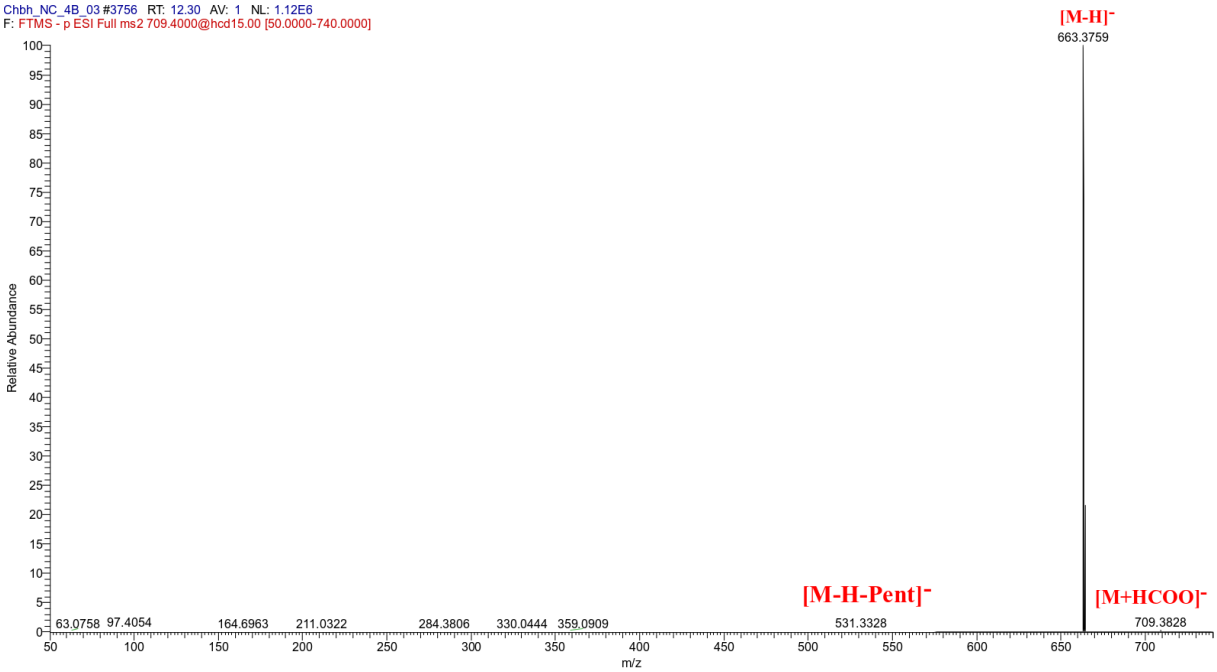

Figure S41: MS^2 spectrum of Compound **32**

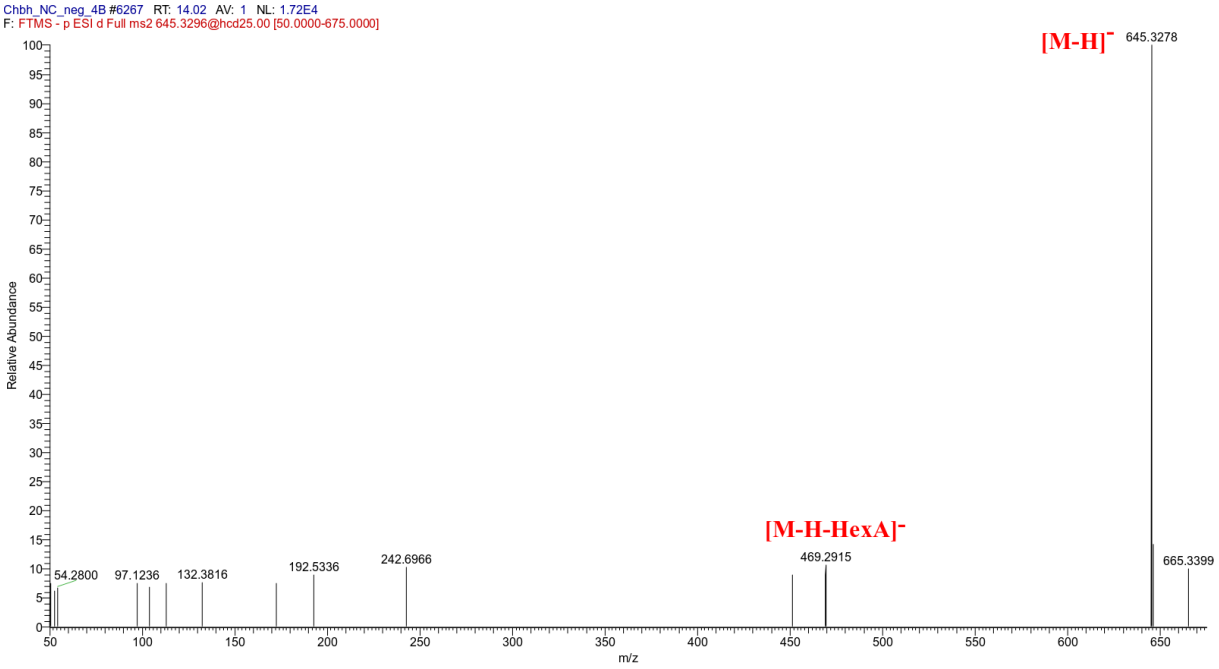

Figure S42: MS^2 spectrum of Compound **33**

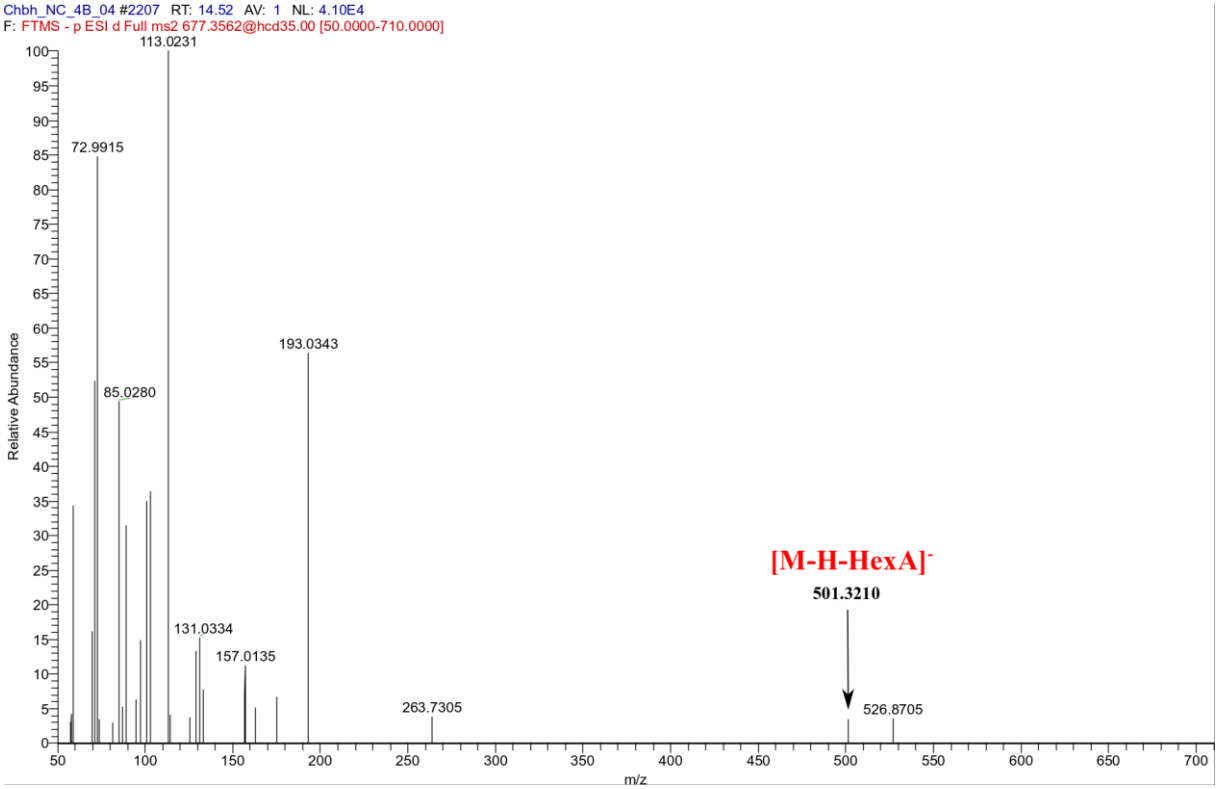

Figure S43: MS^2 spectrum of Compound **34**

Figure S44: MS^2 spectrum of Compound **35**

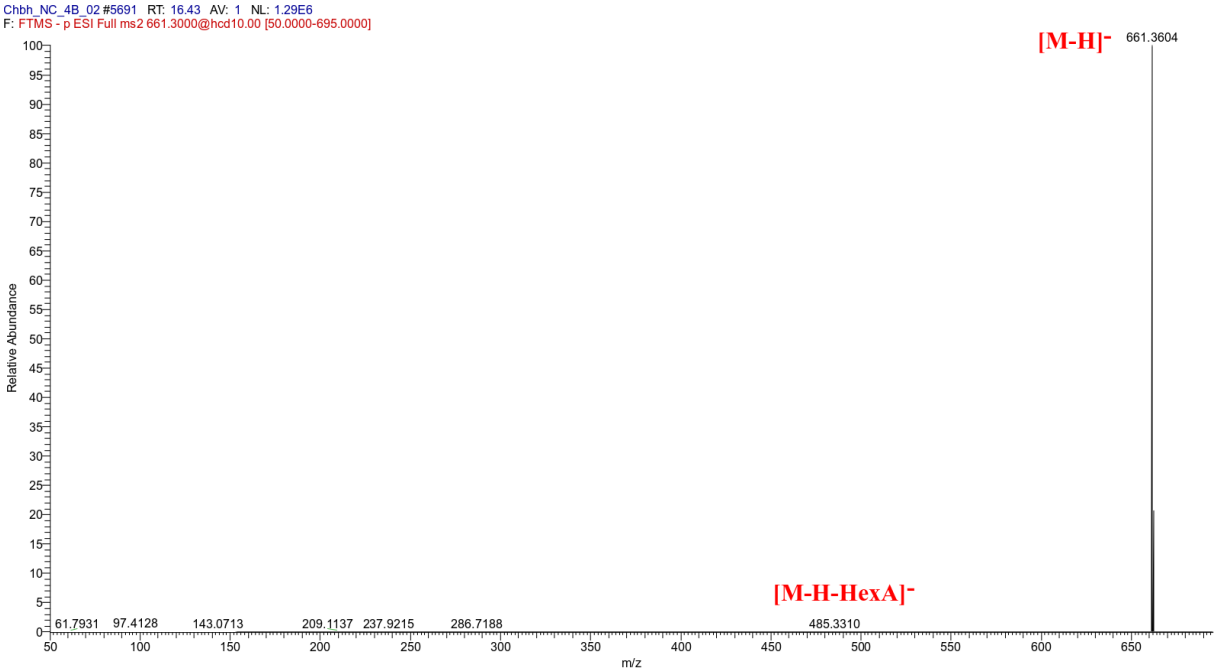

Figure S45: MS^2 spectrum of Compound **36**

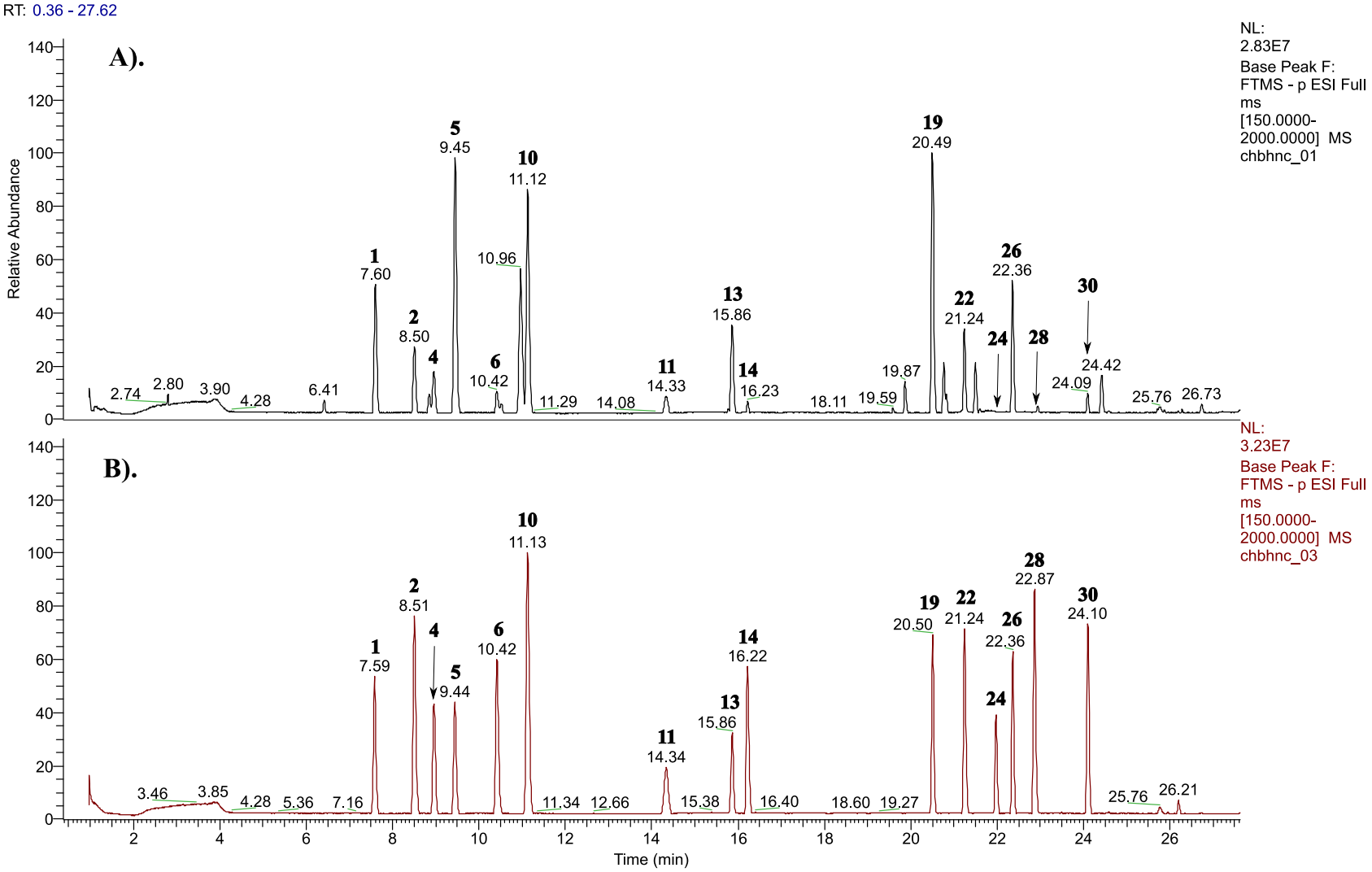

Figure S46: Base peak chromatograms in negative mode of A). the MeOH extract of aerial parts from *C. bonus-henricus* and B). the mixture of reference compounds. The numbering is according to the Table 1.

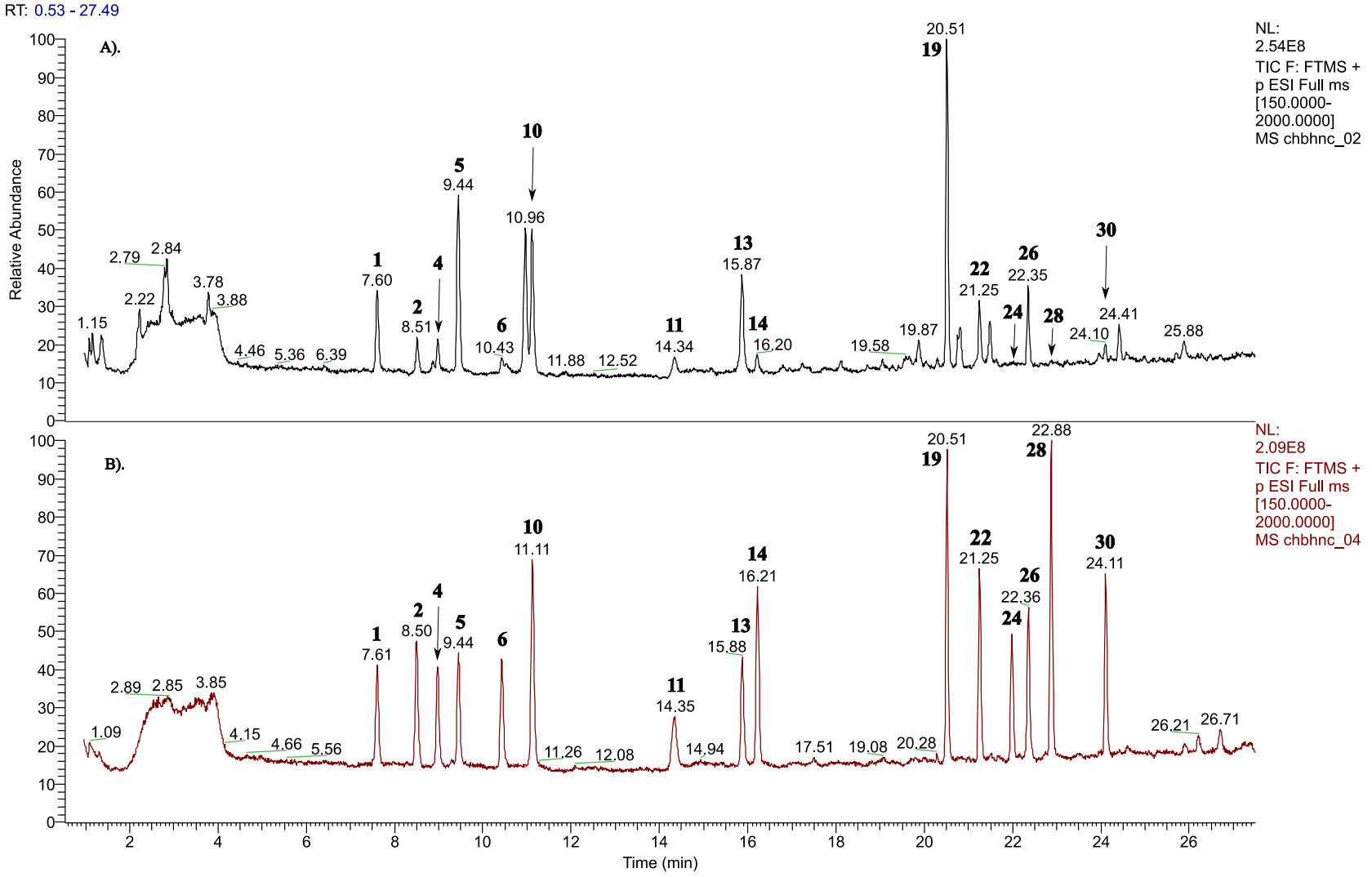

Figure S47: TIC chromatograms in positive mode of A). the MeOH extract of aerial parts from *C. bonus-henricus* and B). the mixture of reference compounds. The numbering is according to the Table 1.